

Continuous atmospheric CO₂, CH₄ and CO measurements at the Observatoire Pérenne de l'Environnement (OPE) station in France from 2011 to 2018

Sébastien Conil¹, Julie Helle², Laurent Langrene¹, Olivier Laurent², Marc Delmotte², Michel Ramonet²

5 ¹DRD/OPE, Andra, Bure, 55290, FRANCE

² Laboratoire des Sciences du Climat et de l'Environnement (LSCE/IPSL), UMR CEA-CNRS-UVSQ, Gif-sur-Yvette, France

Correspondence to: Sébastien Conil (sebastien.conil@andra.fr)

Abstract.

Located in North-East France, the Observatoire Pérenne de l'Environnement (OPE) station was built during the Integrated
10 Carbon Observation System (ICOS) Demonstration Experiment to monitor the greenhouse gases mole fraction. Its continental
rural background setting fills the gaps between oceanic or mountain stations and urban stations within the ICOS network.
Continuous measurements of several greenhouse gases using high precision spectrometers started in 2011 on a tall tower with
three sampling inlets at 10m, 50m and 120m above ground level (agl). Measurement quality is regularly assessed using several
complementary approaches based on reference high pressure cylinders, audits using travelling instruments and sets of
15 travelling cylinders (“cucumber” intercomparison program). Thanks to the quality assurance strategy recommended by ICOS,
measurement uncertainties are within the World Meteorological Organisation compatibility goals for carbon dioxide (CO₂),
methane (CH₄) and carbon monoxide (CO). The time series of mixing ratios from 2011 to end of 2018 are used to analyse
trends and diurnal and seasonal cycles. The CO₂ and CH₄ annual growth rates are 2.4 ppm/year and 8.8 ppb/year, respectively,
for measurements at 120m agl over the investigated period. However, no significant trend has been recorded for CO mixing
20 ratios. The afternoon mean residuals (defined as the differences between midday observations and a smooth fitted curve) of
these three compounds are significantly stronger during the cold period when inter-species correlations are high, compared to
the warm period. The variabilities of residuals show a close link with air mass back-trajectories.

1 Introduction

Since the beginning of the industrial era, the atmospheric mole fractions of long lived greenhouse gases (GHGs) have been
25 rising. Increases in surface emissions, mostly from human activities, are responsible for this atmospheric GHGs build up. For
carbon dioxide (CO₂), the largest climate change contributor, only around half of the additional anthropogenic emissions are
retained in the atmosphere, with the remaining 50% being absorbed by the ocean and the land ecosystems (Le Quéré et al.,
2018). For methane (CH₄) the last ten years are characterised by high growth rates at many observation sites, following a
period of stable mole fractions from 2000 to 2007 (Nisbet et al., 2019; Turner et al., 2019). Monitoring the amount fractions

of these GHG is of primary importance for the long-term climate monitoring but also for the assessment of surface fluxes. Remote and mountain atmospheric measurements are needed to assess background mole fractions because they are performed far from anthropogenic sources and/or are located in the free troposphere. Such « global scale » data are of great value for monitoring the global atmospheric GHG build-up and estimating global scale fluxes. However, they are not designed to capture the regional-scale signals necessary to assess local to regional scale fluxes. The specific purpose of the European Integrated Carbon Observation System (ICOS) is to establish and maintain a dense European GHG observations network to monitor long-term changes, assess the carbon cycle and track carbon and GHG fluxes. Inverse atmospheric methods combining tall tower network measurements and transport models are important tools for assessing surface GHG fluxes exchanged with the biosphere and oceans, and estimating the anthropogenic emissions (Broquet et al., 2013; Kountouris et al., 2018). They also offer independent ways to improve the bottom-up emissions inventories required by the international agreement under the United Nations Framework Convention on Climate Change (Bergamaschi et al., 2018; Leip et al., 2018; Peters et al., 2017). ICOS was established as a European strategic research infrastructure which will provide the high precision observations needed to quantify the greenhouse gas balance of Europe and adjacent regions. It is now a widespread infrastructure made up of three integrated networks measuring GHGs in the atmosphere, over the ocean and at the ecosystem level. Each network is coordinated by a thematic center that performs centralised data processing. One of the key focuses of ICOS is to provide standardised and automated high-precision measurements, which is achieved by using common measurement protocols and standardised instrumentations. In the atmospheric monitoring network, ICOS targets the World Meteorological Organization (WMO) / Global Atmosphere Watch (GAW) compatibility goal (WMO, 2018) within its own network as well as with other international networks. During the preparatory phase from 2008-2013 a demonstration network and new stations were set up with harmonised specifications (Laurent et al ; 2017). The Atmospheric Thematic Center (ATC) performs several metrological tests on the analysers and provides technical support and training regarding all aspects of the in situ GHG measurements (Yver Kwok et al., 2015). The ATC is also responsible for the near real time post processing of the measurements (Hazan, et al., 2016).

The OPE station was established under a close collaboration between the French national radioactive waste management agency (Andra) and the Laboratoire des Sciences du Climat et de l'Environnement (LSCE) as part of the demonstration experiment during 2010 and 2011 in accordance with ICOS atmospheric station specifications. It is a continental regional background station contributing to the network by bridging the gap between remote stations like Mace Head (MHD) or Jungfraujoch (JFJ), and urban stations like Saclay or Heidelberg. The potential of ICOS continuous measurements of CO₂ dry air mole fraction to improve Net Ecosystem Exchange estimates at the mesoscale across Europe was evaluated in Kadygrov et al. (2015). Pison et al. (2018) addressed the potential of the current ICOS European network for estimating methane emissions at the French national scale.

The main objectives of this paper are to describe the OPE monitoring station and the continuous GHG measurements system, to present its performance characteristic and to draw results from the first eight years of continuous operations.

2 Site description and GHG measurements system

2.1 Site location

The OPE atmospheric station (48.5625°N, 5.50575°E WGS84, 395 m asl) is located on the eastern edge of the Paris Basin in the north-east part of France, western Europe, as shown on Figure 1. The landscape consists of undulating eroded limestone plateaus dissected by a few SE-NW valleys (60 to 80m). The station is on top of the surrounding hills in a rural area with large crop fields, some pastures and forest patches. According to Corine Land Cover 2012, the dominant land cover types in the 25 / 100 km surrounding area are Arable land/crops: 39% /44%, Pastures : 14% /18%, Forest : 44% /34%. Based on GEOFLA database from Institut national de l'information géographique et forestière (IGN), the mean population density within a 25 / 100km radius from the station is 26 / 64 (inhab.km⁻²). The closest small towns are Delouze with 130 people located 1 km to the south-east and Houdelaincourt with 300 people located 2km to the south-west. The closest cities are Saint Dizier (45,000 inhabitants) located 40km away to the west, Bar Le Duc (35, 000 inhab.) 30km at the north-west, Toul (25,000 inhab.) 30km to the east and Nancy (450,000 inhab.) 50km to the east. With 20 000 cars/day, the major road is located 15km to the north (RN4). The station includes a 120m tall tower and two portable and fully equipped modular buildings in a 2ha fenced area. The station infrastructure was built in 2009 and 2010 and the measurements systems started in 2011.

15 The OPE station is designed to host a complete set of in situ measurements of meteorological parameters, trace gases (CO₂, CH₄, N₂O, CO, O₃, NO_x, SO₂) and particle parameters(size distribution, absorption and diffusion coefficients, number and mass, chemical composition, radioactivity). The station is part of the French aerosol in situ network contributing to ACTRIS and AERONET program. It is part of the IRSN (Institut de Radioprotection et de Sûreté Nucléaire) network for ambient air radioactivity monitoring. The station also contributes to the French air quality monitoring network and to the European

20 Monitoring and Evaluation Program.



Figure 1: Geographical location of the OPE atmospheric station (left) and aerial photograph illustrating the landscape surrounding the station (right).

2.2 Local meteorology and air mass trajectories

Local meteorology is monitored using three sets of meteorological sensors located at the three measurement levels on the tower (10m, 50m and 120m agl). Standard meteorological parameters, Temperature, Relative Humidity, Pressure and Wind Speed and Direction, are monitored in compliance with ICOS Atmospheric Station specifications. Minute averaged data are logged and used to produce hourly mean fields. In addition there is a ground based weather station operated by Meteo France, the French national weather service providing hourly mean data in compliance with World Meteorological Organization specifications.

The mean annual temperature between 2011 and 2018 was 10.5°C. The minimum temperature was -15.2°C and the maximum temperature was 36.4°C. The cumulated annual precipitation was 829mm on average. Two local wind regimes are predominant, a south-westerly regime and an east-north easterly regime.

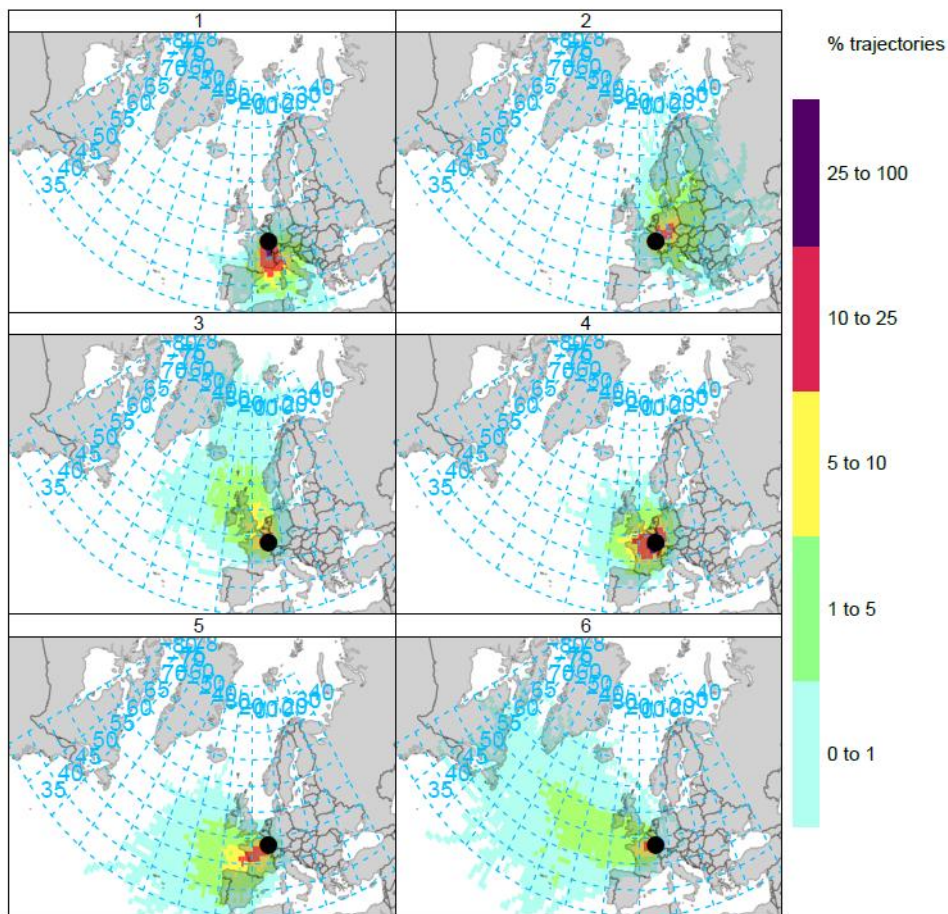


Figure 2: 96hours back-trajectory frequencies reaching the OPE station top level for each of the six clusters identified using the HYSPLIT tools and the NCEP reanalysis for the period 2011-2018.

96h back trajectories were computed for the OPE station top level (120m) using the National Centers for Environmental Prediction (NCEP) reanalysis fields and the HYSPLIT model every 6 hours. As we focus on the afternoon mean residuals (defined as the differences between midday observations and a smooth fitted curve), we only use back-trajectories reaching the OPE station at 12:00 UTC. The clustering tools from HYSPLIT were used to determine the main types of air mass reaching the station. Based on the total spatial variance (TSV) metric, describing the sum of the within cluster variance, the optimal number of clusters was six (lowest number with a small TSV). The TSV plot is shown in Figure S1 of the supplementary material. The six clusters were defined as shown in Figure 2. This figure shows the frequency of trajectories for each cluster passing through the corresponding grid point and reaching the OPE station at 12:00 UTC. Clusters 1, 2 and 3 are characterised by continental air masses (mostly from south, east and north respectively). Cluster 4 is dominated by slow moving trajectories from the west. Clusters 5 and 6 are dominated by western marine trajectories.

2.3 GHG measurements system

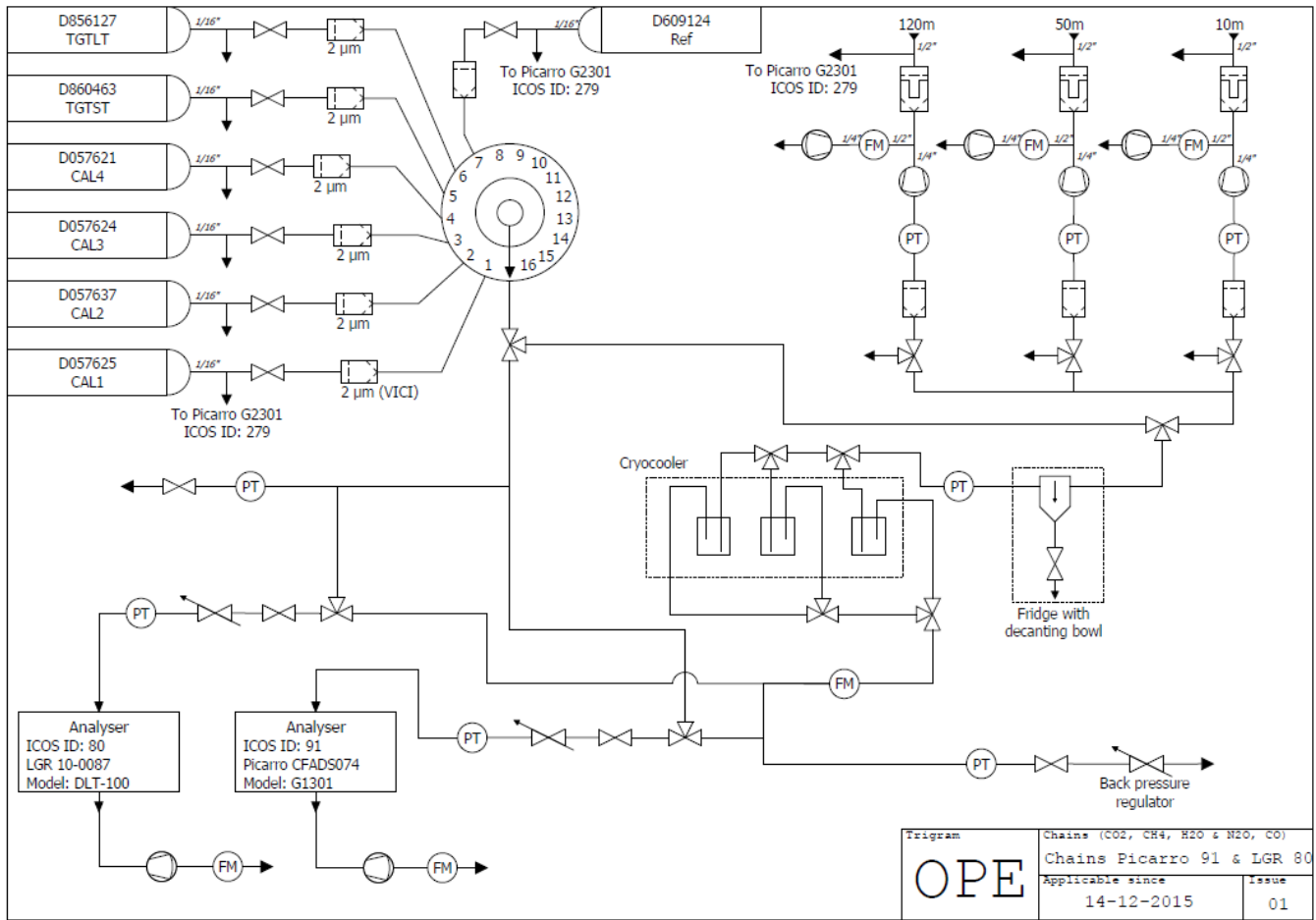
The GHG measurement system was setup in 2011 with support from the ICOS Preparatory Phase projects. It was built in order to comply with the Atmospheric Station class 1 stations specifications from ICOS. It relies on a fully automated sample distribution system with remote control backed up by an independent robust spare distribution system. It includes several continuous analysers for the main GHGs (CO₂, CH₄ and N₂O), a manual flask sampler and specific analysers or samplers for tracers such as radon, CO and ¹⁴CO₂.

The continuous GHG measurement system is made of three main parts: an ambient air sample preparation and distribution component, a reference gases distribution component and a master component which conducts the main analysis sequence and controls the distribution and analysis systems via pressure and flowrate meters. The station flow diagram is described in Figure 3. Ambient air is collected on the tower at the 10m, 50m and 120m levels and brought down to the shelter located at the tower base using 0.5'' outer diameter Dekabon tubes fitted with a stainless steel inlet designed to keep out precipitation. Five sampling lines are installed at 120m, and three are installed at 10m and 50m. From the 120m level, one line is connected to the ¹⁴CO₂ sampler built by Heidelberg University. Another sampling line is used to collect weekly flask samples. The continuous GHG measurements are performed using two independent sampling lines. The last line is a spare line which can be operated in of the event of problems on another line or for temporary additional experiments such as independent audits like those performed in 2011 and 2014. At 10m and 50m, two lines are used for the continuous GHG measurement system. Both of these levels also have a spare line.

At each level, the continuous GHG monitoring system air is flushed from the tower using three Neuberger N815KNE flushing pumps (15 LPM nominal flow rate) and cleaned by two 40 micron and 7 micron Swagelok stainless steel filters. From each sampling line, a secondary KNF N86KTE-K pump (5.5 LPM nominal flow rate) is used to sample and pressurise the air (through a 2 micron Swagelok filter) to be dried and then analysed. A flowmeter is used to monitor air flow in the flushing line and a pressure sensor is used to monitor sampling line pressure. The air sample is pre-dried in a coil passing through a fridge. To further dry the sample, the air passes through a 335mL glass trap cooled in an ethanol bath at -50°C using a dewar.

Once dried in the cryo water traps (-40°C dew point), the air sample is pressure regulated (~1150 hPa abs at the instrument inlet) and directed to the analysers.

The ambient air distribution component is driven by a control/command component, designed around a Programmable Logic Controller (PLC) for selection and distribution of the ambient air sample from the three sampling heights. This distribution component selects an ambient air sample from one of the three levels using three 3-ways solenoid valves and then directs it to the drying system and to the analysers. Once analysed, the air sample flows back to the distribution panel where a back pressure regulator controls the air pressure in the sample line. A pressure sensor monitors the pressure at the analyser inlets and a flow meter monitors the flow rate at the analyser outlets.



10 **Figure 3: Flow diagram of the OPE GHG measurement system (FM: flow meter, PT: Pressure Transducer)**

The control/command component system selects between standards and ambient air, following the PLC's order, as it is responsible for the sequence management and quality control processes. The standard gas distribution component is based on a 16 position Vici Valco valve from which nine ports are connected to the analysers. The pressure of the selected standard gas

or the ambient air sample is adjusted at the analyser inlet by a manual pressure regulator. All the 1/8" or 1/4" stainless steel distributing tubings are over pressurised to avoid any leakage artefact. According to ICOS internal rules, comprehensive leak checks are performed on a yearly basis and after all maintenance operations.

5 The analysers used are Picarro series G1000 and G2000 cavity ring down spectrometers (CRDS) for CO₂, CH₄, H₂O and CO and Los Gatos Research Off-Axis Integrated Cavity Output Spectroscopy -spectrometers for N₂O and CO. Each analyser used at the station first underwent extensive laboratory tests at LSCE during the development of the ICOS Metrology laboratory at ATC (Lebegue et al., 2016, Yver Kwok et al., 2015). These initial tests provide valuable information about the intrinsic properties of the analysers, their precision, stability, water vapour sensitivity and temperature dependence.

10 Over the 2011-2018 period, the reference analysers were a Picarro G1301 (ICOS# 91) which performs CO₂ and CH₄ (and H₂O) mole fractions analyses and a Los Gatos Research DLT100 (ICOS #80) which is used for CO (and H₂O) mole fraction measurements. A redundant pair of parallel instruments have been running either on the main distribution system and /or on the spare distribution system using the same calibration and quality control strategy.

The routine operating sequence includes :

- 15
- Start with a full calibration including four cycles of four standards lasting 8 hours followed by 30min of Long Term target (LTT) and then by 30min of Short Term target (STT),
 - 5 hours of ambient air in cycles of three steps of 20min for the 10m level, 50m level and then 120m level
 - 20min of Reference gas (REF)
 - 5 hours of ambient air in cycles of three steps of 20min of the 10m level, 50m level and then 120m level
- 20
- 20min of STT

During the first years of the ICOS preparatory phase, the calibrations were performed every two weeks. Due to gas consumption issue and following optimization tests, they are now performed every three weeks.

The routine sequence is summarised in Table S1 in the supplementary materials

25 The flushing and stabilisation periods for the standards are 10 minutes meaning that the first 10 minutes of data for each of the standards are rejected. The flushing and stabilisation period for the ambient air samples are 5 minutes meaning that the first 5 minutes of data for each of the ambient air levels are rejected (only 15min of the total 20minutes every hour are available). The raw data are then calibrated using the two or three two or three weekly full calibration and reference working standards following Hazan et al. (2016). Raw data (between 1s and 5s resolution) are aggregated to one minutes and one hour averages.

30 The results presented here are based on validated minute data from mid 2011 to end of 2018.

The calibrations strategy includes four consecutive cycles of the four calibration cylinders sampled for 30 minutes each, the full calibration lasts 8 hours. An archive reference standard gas called Long Term Target (LTT) is injected every two or three weeks for 30 minutes while a common archive reference standard gas called Short Term Target (STT) is injected for 20 minutes every 10 hours. Another short term working standard called Reference (REF) gas is also used every 10 hours to correct short

term variability. The mole fractions of the standard cylinders cover the unpolluted atmospheric range following ICOS Atmospheric Station specifications (Laurent, 2017). The standard gases are supplied via a SCOTT Nickel-plated brass regulator from a 50l Luxfer Aluminium cylinder. Before March 2016, the standard and performance cylinders used were prepared by LSCE and were traceable to WMO scales (CO₂:WMO X2007, CH₄: WMO X2004A , CO: WMO X2014A , N₂O: WMOX2007). Since March 2016, the standard and performance cylinders used have been prepared by the Central Analytical Laboratories of ICOS (CAL) and are traceable to WMO scales (CO₂:WMO X2007, CH₄: WMO X2004A, CO: WMO X2014A, N₂O: NOAA-2006A). STT and REF cylinders are refilled every 6 months by ICOS-CAL. All the measurement data presented here were recalibrated on these scales.

The raw data from the analysers along with the distribution system monitoring parameters are transmitted to the ATC database on a daily basis. Data are then processed following Hazan et al. (2016) including a specific water vapour correction for the remaining humidity, as well as a station specific automatic flagging process. Data products are then generated so that data quality control can be done on a regular basis. Additionally manual flagging is performed by the station's Principal Investigator (PI) on the raw data and on the hourly aggregated data.

Figure 4 gives an overview of the different GHG continuous analysers in operation at the OPE station and their respective time periods. Details on the start and end dates and additional information regarding ancillary instrumentation are in Table S2 in the supplementary material.

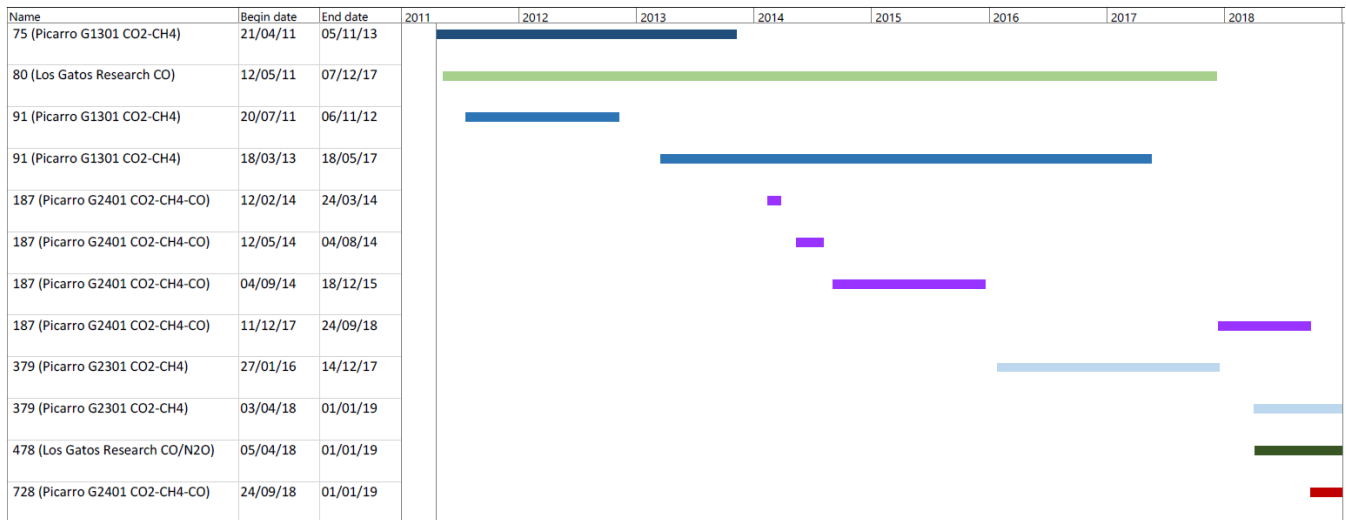


Figure 4: Time diagram showing the different GHG analysers in operation at the OPE station.

2.4 Data processing

The GHG data cover several years and were collected using different sampling systems and analysers. In each of the individual time series, some data are missing because of either sampling issues, analysers problems or local contamination near the station. Very local pollution, for example due to field works or infrastructure maintenance occurs only rarely. Power outages also occurred due to lighting or construction work. Problems on the sampling systems are more frequent and include tube

leaks, pump troubles, filter clogging or control/command component system failure. Analyser problems are also quite common and range from software issues, operating system failures, hardware problems (hard disk, fan, etc.), or worse, liquid contamination (from water or ethanol) of the optical cell.

Raw data from the instruments (mole fractions and internal parameters such as cell temperature/pressure, outlet valve), and from the air distribution system (sequence information and ancillary data such as pressure and flow rates in the sampling lines) are transferred at least once a day to the ATC data server. Data are then processed automatically as described in Hazan et al., (2016). Sequence data are used to generate the ambient air and cylinders raw time series. Mole fractions raw data are flagged automatically using the ancillary data based on a set of parameters defined for each station and instrument. For the Picarro G1301 #91, G2301 #379 and G2401 # 728 analysers, the internal flagging parameters are the same as the ones shown on Table 4 in Hazan et al. (2016). A manual flag is then applied by the station PI in order to eventually discard data using local station information (e.g. local contamination, maintenance operation, leakage, instrumental malfunctions, etc...). The list of descriptive flags available to the PI for valid or invalid data is shown in Table 2 of Hazan et al. (2016). Table 1 below presents the quantitative statistical summary of the raw data status for the different instruments used at the OPE station. Details of the internal flagging associated with the flags presented in this table can be found in Table 6 of Hazan et al. (2016). Flag N corresponds to invalid data rejected automatically. Flags O and K correspond to valid and invalid data, respectively, from the manual Quality Control. Between 62 and 72% of the raw data are valid (O) while around 25% of the raw data are automatically rejected (N), 20% being rejected because of stabilisation/flushing. Corrections related to water vapour content and calibration are then applied. Finally, data are aggregated in time to produce minute, hourly and daily means.

Instrument	Compounds	Start	End	Flag	% raw data
75	CO ₂ /CH ₄	21/04/2011	05/11/2013	O	72.1%
				N	25.80%
				K	2.10%
80	CO	12/05/2011	07/12/2017	O	71.0%
				N	23.5%
				K	5.50%
91	CO ₂ /CH ₄	21/07/2011	22/06/2017	O	67.2%
				N	23.8%
				K	9.00%
187	CO ₂ /CH ₄ /CO	12/02/2014	03/04/2018	O	65.1%
				N	30.7%
				K	4.20%
379	CO ₂ /CH ₄	27/01/2016	31/12/2018	O	71.7%
				N	24.9%
				K	3.40%
478	CO	27/01/2016	31/12/2018	O	62.4%
				N	24.9%
				K	12.70%
728	CO ₂ /CH ₄ /CO	27/01/2016	31/12/2018	O	65.6%
				N	25.0%
				K	9.40%

20 **Table 1: Flags attributed to raw data from the different instruments between mid 2011 and end of 2018. The last two columns provide the type of flag and the percentage of raw data that were attributed this flag. Flagged O data are valid data manually checked, while N and K flagged are non valid data respectively automatically and manually rejected.**

From these individual time series, we built three combined time series for CO₂, CH₄ and CO filling the gaps when possible. The objective is to provide users with continuous time series, combining valid measurements in order to minimise the data gaps. Before merging the time series, each instrument is quality controlled individually, and only measurements which are validated by the automatic data processing and the PI are considered for the combined dataset. For each measurement we indicate the reference of the measuring instrument (unique identifier in the ICOS database), providing the user with analyser traceability. To build these times series from various analyser datasets we used the priority order given in Table 2 for CO₂ and CH₄ and Table 3 for CO. The priority order is defined a priori by the station PI considering which analysers are fully dedicated to the station for long term monitoring purposes. In general secondary instruments are installed for shorter periods to perform specific additional experiments (like dry vs humid air samples, line tests, flushing flow rate tests, etc). For example, 91 was the main instrument for CO₂ and CH₄ followed by 379. While 91 was in maintenance, instruments 75 or 187 were used as spare instruments. At the beginning of 379 operation, 91 was still the main instrument, to maintain time series consistency as long as possible. When 91 operation stopped, 379 became the main instrument. When 379 was in repair, instrument 187 was used as a spare instrument again. For CO, the LGR analyser 80 was the main instrument followed by Picarro G2401 728. When the LGR 80 was out of order, we used either Picarro 187 or LGR 478 as spare instruments. When two instruments are installed for long-term measurements, the priority order should take into consideration the performance of each one. It is the responsibility of the station manager to change the priority list in the ICOS database if needed. Merging the individual time series in such a way implies that the merged time series show steps in their uncertainties as individual analysers have different performance (see Part 3 Data Quality Assessment for details about the steps in repeatability performance).

Compound	Main analyzer	Spare analyzer	Start Date	End Date
CO ₂ / CH ₄		75 (Picarro G1301)	21/04/2011 00:00	20/07/2011 23:00
CO ₂ / CH ₄	91 (Picarro G1301)	75 (Picarro G1301)	21/07/2011 00:00	05/11/2013 23:00
CO ₂ / CH ₄	91 (Picarro G1301)	-	06/11/2013 00:00	11/02/2014 23:00
CO ₂ / CH ₄	91 (Picarro G1301)	187 (Picarro G2401)	12/02/2014 00:00	27/01/2016 00:00
CO ₂ / CH ₄	91 (Picarro G1301)	379 (Picarro G2301)	27/01/2016 00:00	22/06/2017 00:00
CO ₂ / CH ₄	379 (Picarro G2301)	-	22/06/2017 00:00	14/12/2017 00:00
CO ₂ / CH ₄		187 (Picarro G2401)	14/12/2017 00:00	03/04/2018 14:00
CO ₂ / CH ₄	379 (Picarro G2301)	-	03/04/2018 14:00	24/09/2018 14:30
CO ₂ / CH ₄	379 (Picarro G2301)	728 (Picarro G2401)	24/09/2018 14:30	-

20 **Table 2: Order of priority (main vs spare analysers) for CO₂ and CH₄ with ICOS instrument identifiers and associated period**

Various instruments were used in parallel for some time and it is thus possible to assess systematic differences between the data for these common periods. The instruments may have shared sampling tubes, calibration and quality control gases but may have also used different air distribution system and different cylinders. Consequently, differences may occur due to problems associated with time synchronisation, air sampling (sampling and flushing pump efficiencies), calibration and water correction or other causes not yet identified.

Compound	Main analyzer	Spare analyzer	Start Date	End Date
CO	80 (Los Gatos CO/N ₂ O)	-	12/05/2011 00:00	07/11/2012 00:00
CO	80 (Los Gatos CO/N ₂ O)	-	11/03/2013 00:00	12/02/2014 00:00
CO	80 (Los Gatos CO/N ₂ O)	187 (Picarro G2401)	12/02/2014 00:00	18/12/2015 00:00
CO	80 (Los Gatos CO/N ₂ O)	-	18/12/2015 00:00	07/12/2017 00:00
CO		187 (Picarro G2401)	14/12/2017 00:00	05/04/2018 18:00
CO	187 (Picarro G2401)	478 (Los Gatos CO/N ₂ O)	05/04/2018 18:00	24/09/2018 14:00
CO		478 (Los Gatos CO/N ₂ O)	24/09/2018 14:00	24/09/2018 14:30
CO	728 (Picarro G2401)	478 (Los Gatos CO/N ₂ O)	24/09/2018 14:30	-

Table 3: Order of priority (main vs spare analysers) for CO with ICOS instrument identifiers and associated period

Figure 5 shows the afternoon (12:00-17:00 UTC) hourly data difference between the different instruments analysing ambient air at 120m for CO₂ and CH₄. Large deviations in the afternoon means are revealed by such comparison. Summary statistics for the differences shown in Figure 5 for the 120m level (and for the 10m and 50m levels) are given in Table S3 of the supplementary materials. On average, over the full period, the differences at 120m are -0.002 ppm for CO₂ and -0.27 ppb for CH₄, below the GAW/WMO compatibility goals (0.1ppm for CO₂ and 2ppb for CH₄). These significant deviations may come from various sources of uncertainty, such as differing residence time in the sampling systems, water vapour correction, clock issues, or internal analyser uncertainties.

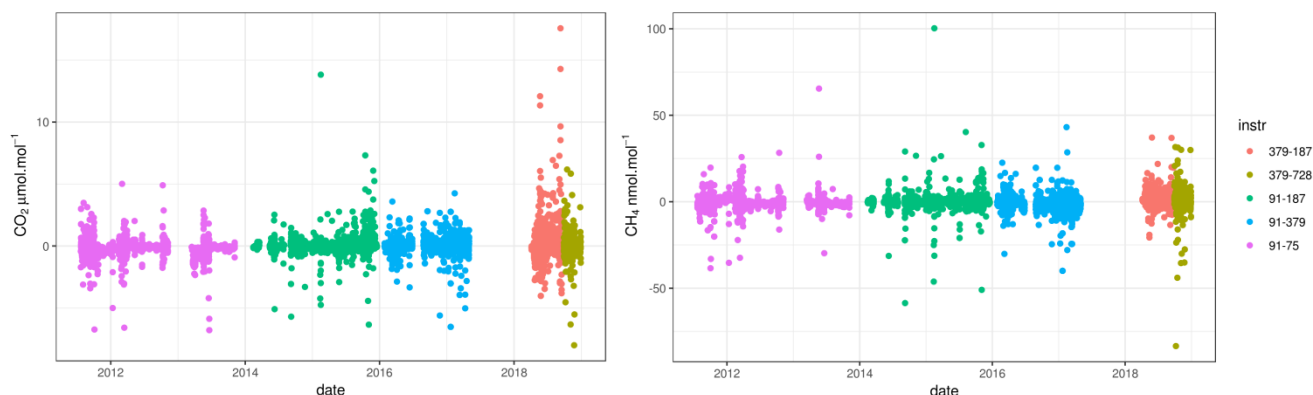


Figure 5: Difference between hourly mean afternoon (12:00-17:00 UTC) data at the top level 120m from the two instruments used at the same time at the OPE station from 2011 to 2018 for CO₂ (left panel) and CH₄ (right panel). The different instruments pairs are shown in colour and their identifiers are labelled in the key by the right panel.

No data filtering was applied regarding the differences and the overall biases are small (Table S3). Large differences can be observed over short periods, especially when the atmospheric signal shows very high variability. For such atmospheric conditions any difference in the time lag between air sampling and measurement in the analyser cell has a significant influence. The persistent presence of a bias between two instruments is used as an indication to perform checks on instruments and air intake chains. For large differences, one of the instruments is generally disqualified based on the tests performed. In the case of moderate differences, the objective is to use this information for estimating uncertainties.

In a similar approach, Schibig et al. (2015) reported results from the comparison between CO₂ measurements from two continuous analysers run in parallel at the JFJ station in Switzerland. The hourly means of the two analysers showed a general good agreement, with mean differences of the order of 0.04 ppm (with a standard deviation of 0.40ppm). However significant deviations of several ppm were also found.

5 3. Data Quality Assessment

QA/QC protocols are applied at several steps in the measurement system. Every day, a conservative quality control is conducted from two complementary standpoints: firstly, intrinsic properties of the spectrometers are verified, and secondly, the sampling system parameters are checked. On a weekly to monthly basis, the field performance of the spectrometers is also checked. A flask program also runs in parallel and is used to expand the atmospheric monitoring to other trace gases and to assess the quality of the continuous measurements. Up to now, flask data were not fully available or were contaminated, and thus have not been used in the present work. A complementary approach to assess compatibility uses round robin or “cucumbers” cylinders circulated between stations within the ICOS European network. Finally, the station compatibility is also assessed during in situ audits using a mobile station and travelling instruments (Hammer et al, 2013, Zellweger et al., 2016).

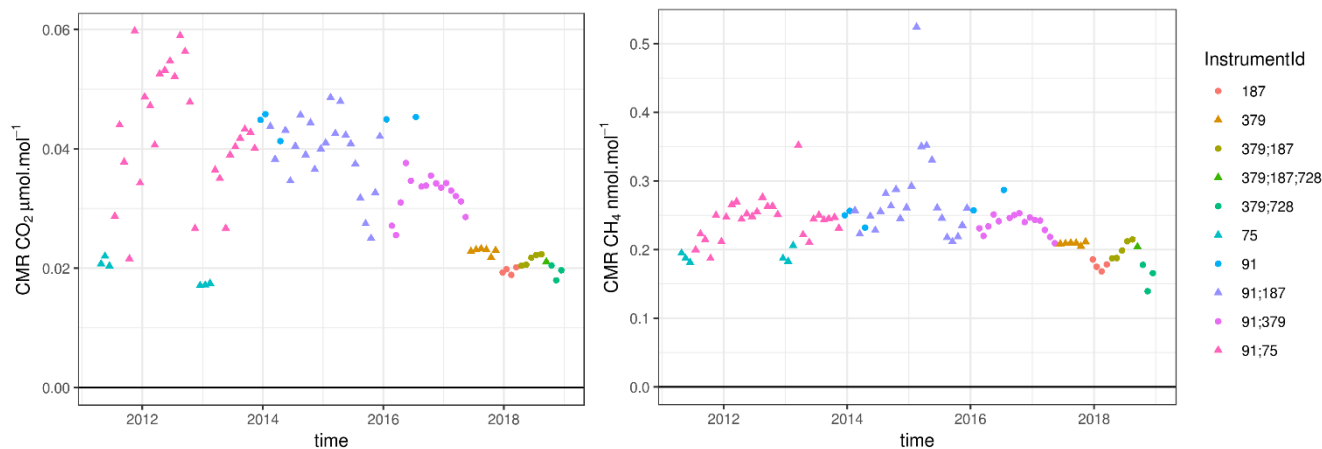
15 In this section we used two metrics defined in Yver Kwok et al. (2015) for quality control assessment of the data. These two metrics are usually calculated under measurement repeatability conditions where all conditions stay identical over a short period. Continuous measurement repeatability (CMR), sometimes called precision, is a repeatability measure applied to continuous measurements. Long-term repeatability (LTR), sometimes called reproducibility, is a repeatability measure over an extended period of time. As ICOS targets the WMO/GAW compatibility goals within its atmospheric network, the analysers must comply with the performance requirements specified in Table 3 of the ICOS Atmospheric Station specifications report (Laurent 2017). ICOS precision limits for CO₂, CH₄ and CO measurements are 50 ppb, 1 ppb and 2ppb respectively. ICOS reproducibility limits for CO₂, CH₄ and CO measurements are 50 ppb, 0.5 ppb and 1ppb respectively.

3.1 Short term target quality control: Field continuous measurement repeatability equivalent

In our basic measurement sequence, the air from a high-pressure cylinder (STT) is analysed twice a day with a ten hours frequency for at least 20 minutes to assess the daily performance of the spectrometers. This metric mainly describes the intrinsic performance of the spectrometers and not of the sampling system. It is a field estimation of the CMR and is computed as the standard deviations of the raw data over 1 min intervals, the first 10 minutes of each target gas injection being filtered out as stabilisation.

Figure 6 shows the monthly mean CMR for the combined time series of CO₂ and CH₄ using the same type of analysers. The time series of CMR for CO are shown in the supplementary materials (Figure S2). For CO₂, we observe a decrease of the CMR over the measurement periods, indicating an improvement in instrument precision. Analyser #91 (Picarro G1301) was shipped

to the manufacturer for a major repair including cell replacement between November 2012 and March 2013. The repair at the Picarro workshop improved the CMR performance of the analyser from more than 0.06 to less than 0.05 ppm. For this instrument, the factory estimated a CMR of 0.04 ppm in 2009 and the lab test at ATC metrology laboratory (MLab) in 2012 estimated a CMR of 0.06 ppm.



5

Figure 6: Monthly mean field Continuous Measurement Repeatability (CMR) for CO₂ (left panel), and CH₄ (right panel) estimated over time for the different instruments in operation at the OPE station over the 2011-2018 period. The different instruments are shown in colour and their identifiers are labelled in the key by the right panel. Some months, have several instruments running at the station and these are identified with several labels.

10 Using a gas chromatograph at the Trainou (TRN) tall tower, Schmidt et al. (2014) found a mean standard deviation in the hourly target gas injections of 0.14 ppm for CO₂, 3.2 ppb for CH₄ and 1.9 ppb for CO for the whole period of 2006-2013. Berhanu et al. (2016) presented their system performance using precision, a metric based on the standard deviation of the 1-min target gas measurements, at 0.05ppm for CO₂, 0.29ppb for CH₄ and 2.79ppb for CO using a Picarro G2401 spectrometer over 19 months from 2013 to 2014. Lopez et al. (2015) presented short term repeatability (a metric similar to CMR) estimates

15 for the gas chromatograph system used at Puy de Dôme (PDD) at 0.1ppm for CO₂ and 1.2 ppb for CH₄, for the years 2010-2013. Table S4 of the supplementary materials summarises this information.

Table 4 presents the comparison of the CO₂ and CH₄ CMR for the instruments #75/91/187/379/728 estimated by the manufacturer and by the ICOS ATC MLab along with the mean values from station measurements over the 2011-2018 period. The station performance of each individual analyser is consistent with its performance estimated at the factory and at the ATC

20 MLab. Performance is maintained over several years and was not disturbed by the station setting.

Analyser	ICOS Id	CO ₂ (ppm)			CH ₄ (ppb)		
		factory CMR	ATC Mlab CMR	Field mean CMR	factory CMR	ATC Mlab CMR	Field mean CMR
Picarro G1301	91	0.04	0.059	0.048	0.27	0.24	0.27
Picarro G1301	75	0.019	0.022	0.02	0.18	0.26	0.22
Picarro G2401	187	0.023	0.026	0.021	0.2	0.28	0.22
Picarro G2301	379	0.025	0.023	0.022	0.23	0.22	0.2
Picarro G2401	728	0.014	0.013	0.014	0.1	0.09	0.08

Table 4: Continuous measurement repeatability (CMR) estimated by the factory, MLab and field means over 2011-2018 for CO₂ (ppm) and CH₄ (ppb). Instrument model and ICOS Identifier are indicated in the first columns.

For CH₄, the factory estimated CMR for instrument #91 in 2009 was 0.27ppb and the initial lab tests at ATC MLab in 2012 estimated CMR for CH₄ at 0.24 ppb. The repair at the Picarro workshop did not modify the CMR performance of the analyser. For each instrument, the CH₄ performance is very stable over the years with very few outliers. The CO performance (CMR and LTR) estimated at the station is compared to the factory and ATC MLab results in Table 5.

Analyser	ICOS Id	CO (ppb)				
		factory CMR	ATC Mlab CMR	Field mean CMR	ATC Mlab LTR	Field mean LTR
Los Gatos N ₂ O and CO	80	0.15	0.06	0.06	0.3	0.4
Picarro G2401	187	6.5	5.7	5.17	1.7	1.18
Los Gatos	478	0.06	0.09	0.05	0.09	0.05
Picarro G2401	728	2.7	2.69	2.76	0.22	0.33

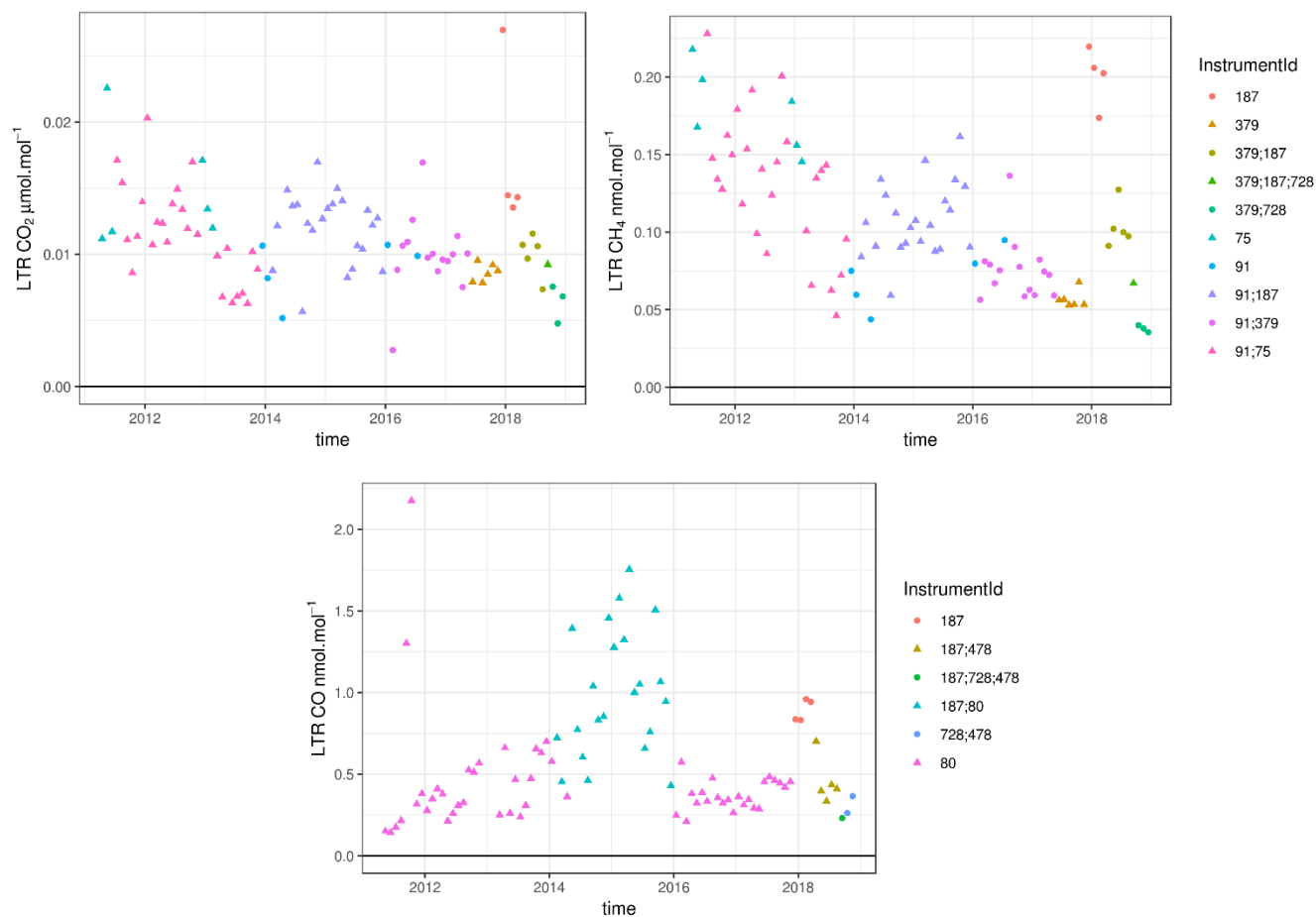
Table 5: Continuous measurement repeatability (CMR) and long-term repeatability (LTR) between factory, MLab and field mean over 2011-2018 of CO (ppb). Their model and ICOS Identifier are indicated in the first columns.

The CMR time series for CO (Figure S2 of the supplementary materials) displays four different periods which are directly linked to the analysers used to build the merged time-series. We used two different types of analyser: one built by Los Gatos Research (instruments #80 and #478) and one built by Picarro (instruments #187 and #728). These two types of analyser have very different internal properties as can be seen in Table 5. The CO CMR results reflect such large differences (shown in Figure S2 of the supplementary materials), the CO CMRs from Los Gatos Research instruments being much lower than the CO CMRs from Picarro. The Picarro 187 and 728 CO LTRs are significantly lower than their CO CMRs. This means that their raw data have large high frequency variabilities but when averaged over several minutes these instruments are quite stable (they are not very sensitive to atmospheric or pressure changes).

Overall the precisions measured at the station for CO₂, CH₄ and CO remain similar to the initial values estimated by the manufacturer and the ATC laboratory, showing no degradation due to the design of the station or the measurement procedures.

3.2 Field long term repeatability

The field LTR is computed as the standard deviation of the averaged STT measurement intervals over 3 days as it is done during the initial test at the ICOS Metrology Lab. Data are then averaged every month. The same STT data are used but with a different perspective, more closely linked to the ambient air data uncertainty.



5

10

Figure 7: Monthly mean field long term repeatability (LTR) for CO₂ (top left panel), CH₄ (top right panel) and CO (bottom panel) estimated over time for the different instruments in operation at the OPE station over the 2011-2018 period. The different instruments are shown in colour and their identifiers are labelled in the keys of the top and bottom panels. Some months have several instruments running at the station and these are identified with several labels.

15

Figure 7 shows the monthly mean field LTR of the merged time series using the different instruments and sampling systems. This figure shows the uncertainties of the data related to the analysers (not the sampling systems). As for CMR, CO₂ and CH₄ LTR show decreasing trends suggesting an improvement of the internal performance of the spectrometers built by Picarro, of the air distribution system and data selection/flagging. The early part of 2018 experienced a markedly worse LTR compared to neighbouring months. This is mostly due to the use of instrument #187, which has relatively poor performance compared to other instruments.

Analyser	ICOS Id	CO ₂ (ppm)		CH ₄ (ppb)	
		ATC Mlab LTR	Field mean LTR	ATC Mlab LTR	Field mean LTR
Picarro G1301	91	0.02	0.01	0.08	0.08
Picarro G1301	75	0.01	0.01	0.21	0.17
Picarro G2401	187	0.02	0.02	0.22	0.17
Picarro G2301	379	0.007	0.009	0.1	0.06
Picarro G2401	728	0.005	0.008	0.06	0.02

Table 6: Long term repeatability (LTR) of CO₂ (ppm) and CH₄ (ppb) estimated by MLab and field mean over 2011-2018. Instrument model and ICOS Identifier are indicated in the first columns.

The comparison of the field mean LTR and ATC MLab LTR for the different instruments are shown in Table 6 for CO₂ and CH₄. The LTR field performance of the analysers are consistent with their initial assessments. Periods of lower CO₂/CH₄ LTR are associated with instruments #91, #379 or #728 while periods with higher CO₂/CH₄ LTR are associated with instruments #75 or #187.

As for CMR, the CO LTR monthly time series shows four different periods but with a smaller contrast, associated with the type of analyser used at the station. Most periods with LGR instruments (#80 or #478) show a LTR under 0.7 ppb while periods with Picarro instrument #187 show a LTR above 0.5 ppb.

Different periods have different uncertainty levels related to instrument performance. While Los Gatos Research instruments show lower CO LTRs they have stronger temperature sensitivities generating high short-term variability in conditions where the temperature is not well controlled. Corrections for these temperature induced biases required the frequent use of a working standard.

15 3.3 Station audit by travelling instruments

A metric such as CMR is very useful for monitoring the internal performance of instruments and for identifying any instrument failure as early as possible. Other instrument related metrics such as calibration long term drift or calibration stability over the sequences are also useful for monitoring instrument performance. However, they do not give an assessment of the overall measurement systems. Flask versus in-situ comparisons, or station audit by travelling instruments are recognised as essential tools in the performance and compatibility assessment of a measurement system. ICOS audits are performed by a mobile lab, hosted by the Finnish Meteorological Institute in Helsinki, and equipped with state of the art GHG analysers and travelling cylinders. The measurements data from the station are centrally processed at the ATC. However, the data produced by the Mobile Lab are computed separately to maintain the independent nature of the Mobile Lab and at the same time to evaluate the performance of the centralised data processing.

25 The OPE station was audited twice, once in summer 2011, soon after the station was set up, during the feasibility study for the travelling instrument methodology and then in summer 2014, when the ICOS Mobile Lab was ready for operation. During the two week intercomparison in 2011, significant differences for CO₂ and CH₄ were noticed between the Fourier Transform

Infrared (FTIR) travelling instrument and the CRDS reference instrument (Hammer et al., 2013). As the two instruments have different temporal resolutions and different response times, the CRDS measurements were convoluted with an exponential smoothing kernel representing a 3 min turn-over time to match the FTIR specifications. For CO₂ the smoothed differences vary between 0.1 and 0.2 ppm with a median difference of 0.13 ppm and a scatter of the individual differences of approximately ±0.15 ppm. The smoothed CH₄ differences decrease from 0.7 ppb initially to 0.1 ppb, the median difference being 0.4 ppb. Such large differences were caused by relatively poor performance of the CRDS and FTIR instruments because of specific hardware problems and also due to the large temperature variations (10 K) within the measurement container. During the summer of 2011, the travelling instrument was also set up at the Cabauw (CBW) station in the Netherlands. The audit showed better instrument performance but the same kind of differences for ambient air comparisons. While the CO₂ deviations at CBW were partly explained by a travelling instrument intake line drawback and by calibration issues on the main measurement system, at OPE no final explanation has been found for the observed differences.

In the summer of 2014, the two months audit was performed using a Picarro G2401 travelling instrument and a FTIR. However the FTIR performance was not yet optimised and the difference in time resolution made it difficult to use it properly. Results from this instrument are not considered here. On average, the OPE standard cylinders analysed by the travelling instrument showed 0.03 ppm and 0.10 ppm higher CO₂ mole fractions at the beginning and at the end of the audit, respectively, than the assigned values used to calibrate measurements at OPE. Similar results were found for CH₄ with relatively low differences ranging between 0 and 1 ppb. The instruments and the working standards (OPE and travelling standards) were calibrated against two different sets of standards, introducing biases in the measurements of cylinders and of ambient air. The intercomparison was complicated by the fact that the station was struck by lightning three times during the summer, causing major power outages and electrical damage to the infrastructure. Such power outages generate shifts in the CRDS analyser response that prevent drift correction of the calibration response, degrading analyser performance. The ambient air comparison was based on two sampling lines, one line delivering dry air samples to Picarro G1301 #91 and wet air samples to Picarro G2401 #187, and one independent line for the audit supplying wet air samples to the travelling instrument (TI). The wet air measurement data from analyser #187 data were corrected for water vapour by the factory Picarro correction, but the TI wet air measurement data were corrected by an improved water correction based on water droplet test performed at the beginning of the intercomparison using a simplified version of the Method #2-EMPA implementation presented in Rella et al. (2013). The ambient air CO₂ mole fractions measured in dry and wet air samples by the OPE analysers showed lower mole fractions compared to the TI measurements, by 0.10 ppm at the beginning of the audit, and 0.13 ppm at the end. Most of the differences in ambient air measurements can be explained by the bias in the reference scales.

When averaged over the whole period the OPE minus TI measurements differences remain within the WMO/GAW compatibility goal. The OPE Picarro G1301 #91 dry air measurements deviated on average by -0.05 ppm compared to the travelling Picarro G2401 wet air measurements in the case of CO₂, and by 0.70 ppb in the case of CH₄. Similarly the OPE Picarro G2401 #187 wet air measurements differ from the travelling instrument wet air measurements by -0.03 ppm and 1.80

ppb for CO₂ and CH₄, respectively. The CO comparison was carried out for OPE-LGR and OPE-G2401 instruments and compared to the TI G2401: the average deviations exceeded the WMO/GAW component compatibility goal (± 2 ppb).

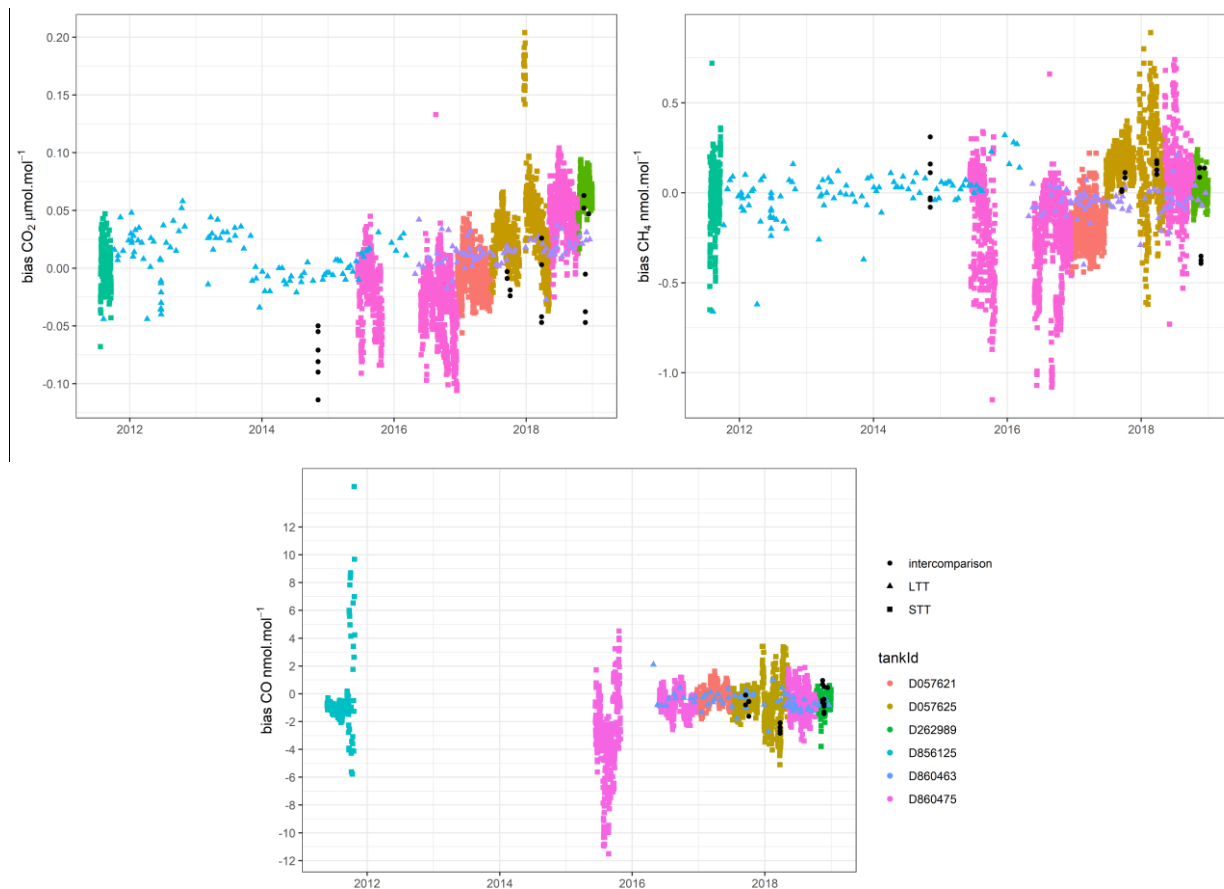
Vardag et al. (2014) presented similar intercomparison results at MHD over two months in spring 2013. For CO₂, the difference between the TI and the station analyser (Picarro G1301) for ambient air measurements at MHD was 0.14 ± 0.04 ppm. During
5 this intercomparison there were no calibration issues as the same set of calibration cylinders was used on both systems. However there could also have been a bias in the water correction effect. Still, most of the differences between station data and the TI during ambient air measurements remained unexplained. These results and the previously published results highlight the major difficulties that station PIs are facing with intercomparison interpretation and understanding. Upcoming sampling line tests, which are mandatory in the ICOS network at least on a yearly basis, may help us understand if the sampling design
10 introduces artefacts.

3.4 Travelling “Cucumbers” cylinders and station target tank biases

At the beginning of station operation, quality control tanks, or targets, were not systematically used or calibrated. Calibrated tanks were used systematically from 2015 as working standards in order to monitor biases.

In addition the OPE station took part in the CarboEurope « Cucumber » program in the EURO2 loop at the end of 2014, as
15 well as in the ICOS program which started in September 2017. The aim of these programs is to assess measurement compatibility and to quantify potential offsets in calibration scales within a network. The results of these two sequences of « Cucumbers » intercomparison are shown in Figure 8 along with the biases estimated for the station quality control cylinders. The biases estimated from the target tanks operated at the station and the blind Cucumber intercomparison biases are consistent for all species. CO₂ biases are found to be between -0.1 ppm and 0.1 ppm most of the times except for some outliers that still
20 need to be understood. A slight trend may be present in the LTT CO₂ biases between 2014 and 2018. The STT results may show a trend as well but step changes are also present. We attribute the CO₂ biases signal to the convolution of step changes and an interannual trend. The step changes may be due to cylinder changes. The possible CO₂ trend shown by the LTT (of the order of $+0.02$ ppm) remains unexplained at this stage. The re-evaluation of the CO₂ mole fractions of calibration tanks at the ICOS central facility could show a drift in their values, which would lead to a correction of the time series.

25 CH₄ biases are between -0.75 ppb and 0.75 ppb for most cases. CO biases show a large spread at the beginning of station operation partly related to the temperature sensitivity of the Los Gatos Research analyser and the poor temperature control of the measurements container. Since 2016 the CO biases stay within the -5 ppb/ $+5$ ppb range.



5 **Figure 8 Target tanks biases over time for several tanks for CO₂ (top left panel), CH₄ (top right panel) and CO (bottom panel). The Short Term Target (STT), Long Term Target (LTT) and “Cucumbers” intercomparison biases are shown in coloured squares, coloured triangles and black circle. The different colours are related to the different tanks used at the OPE station for quality control.**

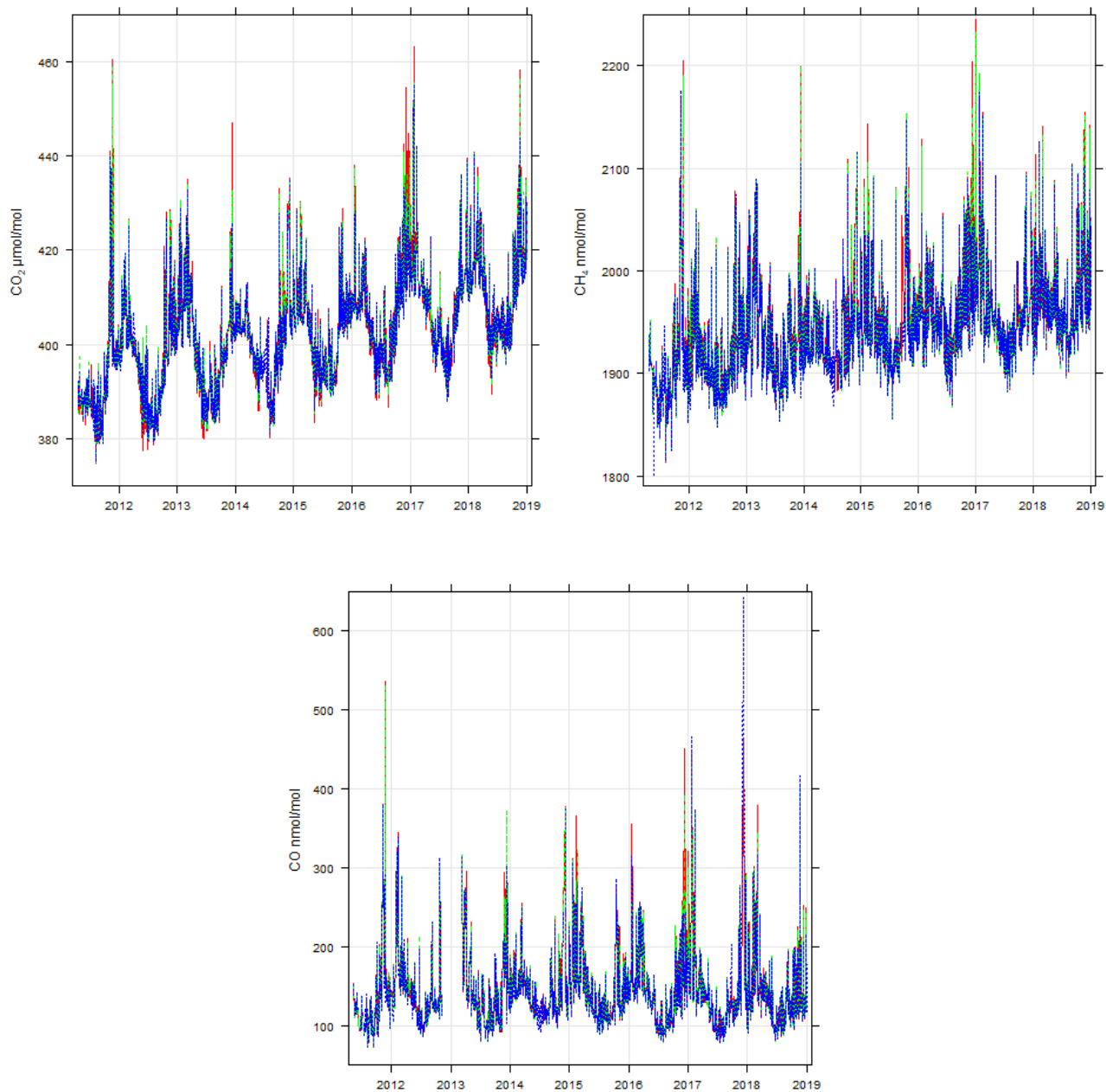
4. Results

Tall tower GHG mole fraction time series over mid latitude continental areas exhibit strong variations from hours to weeks, seasonal and interannual time scales and even longer. Such variabilities are linked to local, regional and global meteorological variations, as well as land biosphere processes and human activities. We will first show the general characteristics of the time series. We will then analyse and show the diurnal cycles computed from the despiked hourly data. We will select only stable situations with low fast variability to focus on the regional scale and compute afternoon means for CO₂, CH₄, CO at the three sampling levels. The seasonal cycles and long-term trends will then be analysed and presented.

10

4.1 General characteristics of the CO₂, CH₄, and CO time series

Figure 9 shows the general characteristics of the afternoon mean mole fractions for CO₂, CH₄, CO at the OPE station at 10m, 50m and 120 m above ground level.



5

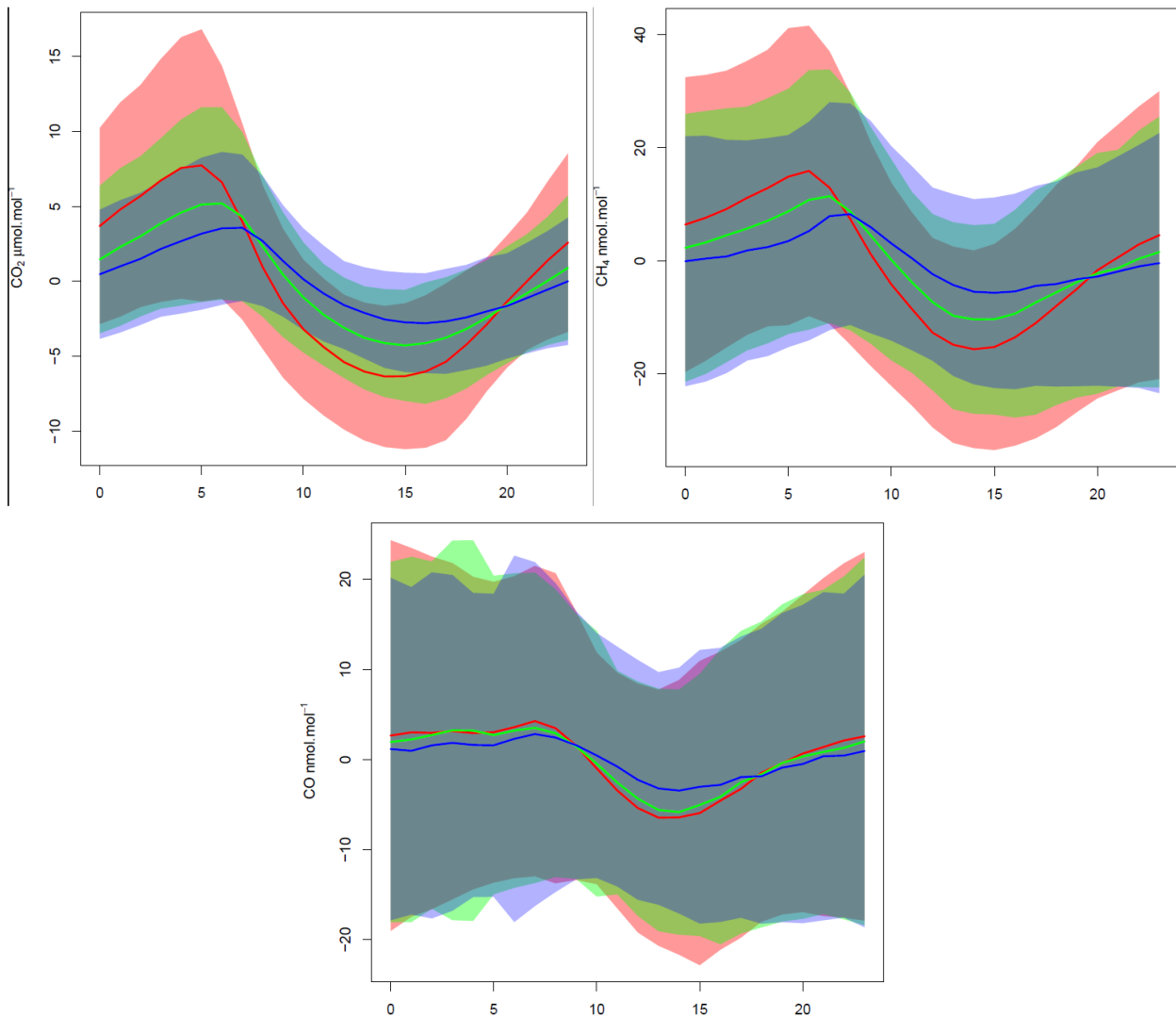
Figure 9: Afternoon (12:00-17:00 UTC) mean CO₂ (top left panel), CH₄ (top right panel) and CO (bottom panel) mole fractions measured at the OPE station at 10m (red), 50m (green) and 120m (blue).

From the summer of 2011 to the end of 2018, the afternoon mean CO₂ at 120m varied from 375 ppm to a maximum of 455 ppm. Over this seven year period, the afternoon mean time series show synoptic variations as well seasonal variations and interannual trends. Similar patterns were observed at several other long term monitoring stations in western Europe over different periods (Popa et al., 2010, Vermeulen et al., 2011, Schmidt et al., 2014, Lopez et al., 2014, Schibig et al., 2015, Satar et al., 2016, Stanley et al., 2018, Yuan et al., 2019). At European background stations such as the MHD coastal station or mountain stations (JFJ, Zugspitze-Schneefernerhaus ZSF or PDD) the interannual times series are dominated by long term trends and seasonal changes. At regional continental stations (CBW, TRN or Bialystok BIK), the synoptic variations have a much larger intensity due to the proximity of strong continental sources. The patterns and amplitude of synoptic variations and of seasonal changes depend on the sampling height, the lowest level (10m) having a higher variability than the highest level (120m). Vertical gradients of CO₂ are present year round but are stronger in summer and weaker in winter, and the gradient variability is much stronger in summer.

The time series for CH₄ afternoon mean mole fractions are also characterised by a long term trend with a weaker seasonal cycle. Synoptic variations can be as high as 150 to 200 ppb on hourly time scales and are stronger at the lowest level. Vertical gradients of CH₄ are present year round and show a small seasonal cycle. The time series CO afternoon mean mole fractions do not show any long-term trend but are characterised by strong seasonal cycles. Synoptic variations can be as high as 200 ppb on hourly time scales and are stronger at the lowest level. Vertical gradients of CO are much stronger in winter and weaker in summer.

4.2 Diurnal Cycles and vertical gradients

The diurnal cycles of trace gases result from atmospheric dynamics (especially the daily amplitude of the boundary layer height), surface fluxes and atmospheric chemistry. The mean diurnal cycles of CO₂, CH₄ and CO are shown in Figure 10 for the three sampling levels (10m, 50m and 120m). Despiked hourly data (not detrended or deseasonalised) were used to compute the mean diurnal cycles. CO₂, CH₄ and CO mole fractions displays similar diurnal cycles due to the similar atmospheric dynamics control: large increase of mean mole fractions and vertical gradient during night-time in contrast with a reduction of mean of mole fractions and vertical gradients during daytime. During the afternoon, while the CH₄ and CO mole fractions at the lowest level stay larger than those at the top level, the CO₂ mole fractions at the lowest level are slightly lower than those at higher level. This CO₂ depletion is due to vegetation growth and photosynthesis (which are stronger in summer and almost disappear in winter). The diurnal cycles of CO₂ and CH₄ are larger in spring and summer while for CO it is larger in winter.



5 **Figure 10 Mean diurnal cycles of CO₂ (top left panel), CH₄ (top right panel) and CO (bottom panel) for the three sampling levels 10m (red), 50m (green) and 120m (blue), computed over the period 2011-2018. The shaded areas correspond to the + and - 1 standard deviations around the mean diurnal cycles.**

For the three compounds, the vertical gradients are much stronger at night, and the highest mole fractions are measured near the ground. During the day, the gradients almost disappear, mainly because of the enhanced vertical mixing of the lower atmosphere. In spring and summer, the CO₂ afternoon mole fraction at the lowest level is slightly below that at the highest level reflecting the photosynthesis pumping of CO₂ by plants. Vertical CO₂ gradients build up again in the late afternoon.

10 In the warm period (from May to September), the mean vertical gradient of CO₂ is 0.4 ppm during the afternoon (12:00-17:00 UTC) and -9.95 ppm at night (00:00-05:00 UTC). During the cold period (from October to April) the mean vertical gradient of CO₂ is -0.24 ppm during the afternoon (12:00-17:00 UTC) and -3.5 ppm at night (00:00-05:00 UTC). Similar patterns were

observed at CBW, for the 1992 -2010 period but with stronger amplitude (Vermeulen et al., 2011). Stanley et al. (2018) showed the vertical gradients of CO₂ and CH₄ mole fractions at two tall towers in the United Kingdom (UK). Daytime vertical differences of CO₂ were very small (<1ppm) (positive in winter and negative in the other seasons). Night-time vertical gradients of CO₂ were always negative between 3 ppm and 8 ppm.

5 In the warm period the mean CH₄ vertical gradient is -0.5 ppb during the afternoon (12:00-17:00 UTC) and -20.7 ppb at night (00:00-05:00 UTC). In the cold period the mean CH₄ vertical gradient is -4 ppb during the afternoon and -18.5 ppb at night. Similar patterns and amplitudes were shown in the UK by Stanley et al. (2018). Vermeulen et al. (2011) also presented similar patterns but with larger amplitudes, the CBW vertical gradients of CH₄ reaching -300 ppb during summer between the 20m and 200m levels.

10 **4.3 Regional scale signal extraction**

The station time series exhibit strong variability from hourly to interannual time scales. These variations may be related to meteorological variability and to variations in sources and sinks. We are mostly interested in the regional signatures at scales that can be approached using model inversions and assimilation tools. For this reason, we want to isolate the situations where the local influence is dominant and shadows the regional signature from the time series and data aggregation. We then need to

15 define the background signal to which the regional scale signal is added.

Such local situations and background definitions may be extracted purely from time series analysis procedures, or may be constrained on a physical basis. El Yazidi et al. (2018) assessed the efficiency and robustness of three statistical spikes detection methods for CO₂ and CH₄ and concluded that the two automatic methods, namely Standard Deviations (SD) and Robust Extraction of Baseline Signal (REBS) could be used after a proper specification of parameters. We used the El Yazidi et al.

20 (2018) method on the composite merged minute time series to filter out « spike » situations. From the despiked minute data we built hourly means, which were used to analyse the diurnal cycles. Focusing on data with regional footprints, we selected only afternoon data with low hourly variability when the boundary layer is larger and the vertical mixing is more efficient. We excluded data showing large variations by using the minute standard deviations. Hourly data with minute standard deviations larger than the three interquartile range computed month by month were excluded from the afternoon mean, leading to a

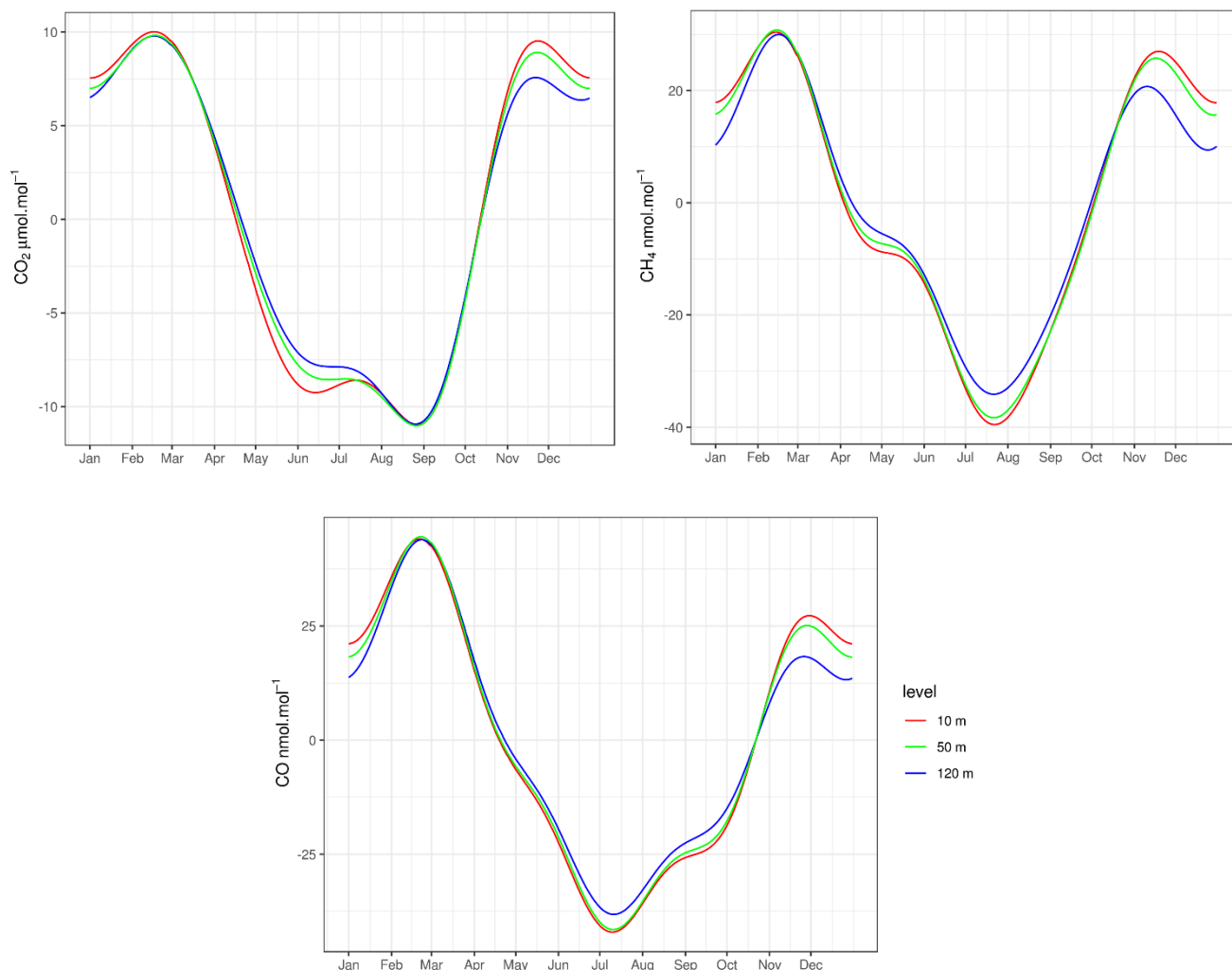
25 rejection of 2.9 % to 4.2% of the hourly means of CO₂, CH₄ and CO.

We then used the CCGCRV curve fitting program from NOAA (Thoning et al., 1989) with the standard parameters set (npoly=3, nharm=4) to compute the mean seasonal cycles and trends for the three compounds. CCGCRV results were compared with similar analysis performed using the R package, Openair (Carslaw and Ropkins, 2012) for the seasonal cycle and the trend using the Theil-Sen method (Sen, 1968).. We then computed the afternoon mean residuals from the seasonal

30 cycle and trends using the CCGCRV results.

4.4 Seasonal cycles

Erreur ! Source du renvoi introuvable. shows the mean seasonal cycles of CO₂, CH₄ and CO at the three measurement levels (10m, 50m and 120m agl). Each of the three GHGs displays a clear seasonal cycle, with higher amplitudes at the lower sampling levels. Minimum values are reached during summer when the boundary layer is higher and the vertical mixing is more efficient. In addition to the boundary layer dynamics, the seasonal cycle of the surface fluxes and the chemical atmospheric sink also play significant roles. The correlations of dynamic and flux processes at the seasonal scale make it difficult to distinguish the role of each process. CO₂ vertical gradients are observed in late autumn / early winter when the CO₂ mole fractions at 10m are larger than at 120m.



10

Figure 11: Mean seasonal cycles of the afternoon data at the three measurement levels (10m in red, 50m in green and 120m in blue) for CO₂ (top left panel), CH₄ (top right panel) and CO (bottom panel) computed over the 2011-2018 period using CCGCRV.

Minimum values are reached in late summer for CO₂, around the end of August with no vertical gradients around this minimum. Vertical gradients appear in late spring with a maximum gradient in June when a secondary minimum is observed at the lowest level but not at the higher levels. The amplitude of the CO₂ seasonal cycle is nearly 21 ppm at the three levels. The CO₂ seasonal cycle amplitudes observed at BIK and CBW were between 25ppm and 30ppm depending on sampling height (Popa et al., 2010; Vermeulen et al., 2011). The two early and late summer CO₂ minima were also observed by Haszpra et al. (2015), at the Hegyhatsal tall tower in western Hungary between 2006 and 2009, and their timings are very close to those of OPE. But only one summer minimum between August and September was observed at the BIK (Popa et al., 2010), CBW (Vermeulen et al., 2011) and TRN tall towers (Schmidt et al., 2014) and at the Schauinsland (SSL) and ZSF mountains stations (Yuan et al., 2019). Ecosystem CO₂ flux measurements performed in 2014 and 2015 near the OPE atmospheric station revealed that the forest and grassland Net Ecosystem Exchange had two maxima in early summer and late summer with a decrease in between (Heid et al., 2018). The two early and late winter maxima were also observed by Popa et al. (2010) at the BIK tall tower with similar timings, end of November and February. But only one winter maxima was observed in January at CBW (Vermeulen et al., 2011), TRN (Schmidt et al., 2014) and Hegyhatsal (Haszpra et al., 2015), in February at SSL and in March at the ZSF mountain station (Yuan et al., 2019).

At OPE minimum CH₄ values are observed in July and maximum values are reached in February and November. The peak-to-peak amplitude of the CH₄ seasonal cycle is nearly 70 ppb at the three levels. At BIK, there was only one maximum in December and minimum values were reached between May and June (Popa et al., 2010). The seasonal cycle amplitude was between 64 and 88 ppb. At CBW, CH₄ mole fractions peaked at the end of December and were at minimum at the end of August. The seasonal cycle amplitude was between 50 ppb and 110 ppb depending on the sampling level (Vermeulen et al., 2011).

The CO seasonal cycle peaks at the end of February, with a secondary peak at the end of November. Minimum values are reached in July, earlier than the CO₂ and CH₄ minimum. The peak-to-peak amplitude of the CO seasonal cycle is between 80ppb and 90ppb. At BIK, the CO maximum was reached in January (with a delay compared to CO₂ and CH₄) and minimum values were observed in June, with a peak to peak seasonal cycle amplitude between 130ppb and 200ppb (Popa et al., 2010). At CBW, the CO maximum was reached in January (also with a delay compared to CO₂ and CH₄) and minimum values were observed in August. The peak to peak CO seasonal cycle amplitude varied between 90ppb and 130ppb (Vermeulen et al., 2011).

4.5 Trends

Table 7 reports the mean atmospheric growth rates computed for the three compounds at the top level using the CCGCRV and Theil-Sen approaches. The mean annual growth rate of CO₂ over the 2011-2018 period is 2.5 ppm/year using the Theil-Sen method and 2.3 ppm/year using CCGCRV. This is consistent with the Mauna Loa global station rate which is also 2.4 ppm/year on average for the period 2011-2018. It is stronger than the growth rate reported for the ZSF mountain station: 1.8ppm /year,

over 1981-2016 (Yuan et al., 2019), and for the CBW station: 2.0 ppm/year, over 2005-2009 (Vermeulen et al., 2011). Such comparisons are only qualitative and must be used with caution, as the time periods considered are different. However, they suggest that the atmospheric CO₂ growth may speed up in the European mid-latitudes.

OPE-120m	CO ₂ (ppm)	CH ₄ (ppb)	CO (ppb)
CCGCRV 2011-2018	2.35 (1.93 ; 2.77)	8.85 (7.35 ; 10.34)	-0.22 (-3.9 ; 3.5)
Theil-Sen2011-2018	2.54 (1.92 ; 3.28)	8.91 (7.64 ; 9.96)	-0.49 (-1.71 ; 0.73)

5

Table 7: Growth rates of CO₂, CH₄ and CO mole fractions at OPE 120m level for the period 2011-2018 computed on the afternoon mean data using the CCGCRV and Theil-Sen methods. 95% confidence intervals are displayed for each compound and method.

The OPE mean CH₄ annual growth rate over the 2011-2018 period is 8.8 ppb/year using CCGCRV and 8.9 ppb/year using the Theil-Sen method. It is slightly larger than the annual increase in Globally-Averaged Atmospheric Methane from NOAA which is 7.5 ppb /year over the 2011-2017 period. A slightly decreasing non-significant trend is seen for CO at OPE over the 10 2011-2018 period. This finding is consistent with recent observations in Europe and in the US. After a global decrease since the end of the 1980s, CO decrease has declined for several years after reaching values below 0.2 ppm at some European background sites such as MHD or JFJ (Lowry et al., 2016, Novelli et al., 2003; Zellweger et al., 2009).

4.6 CO₂, CH₄ and CO residuals

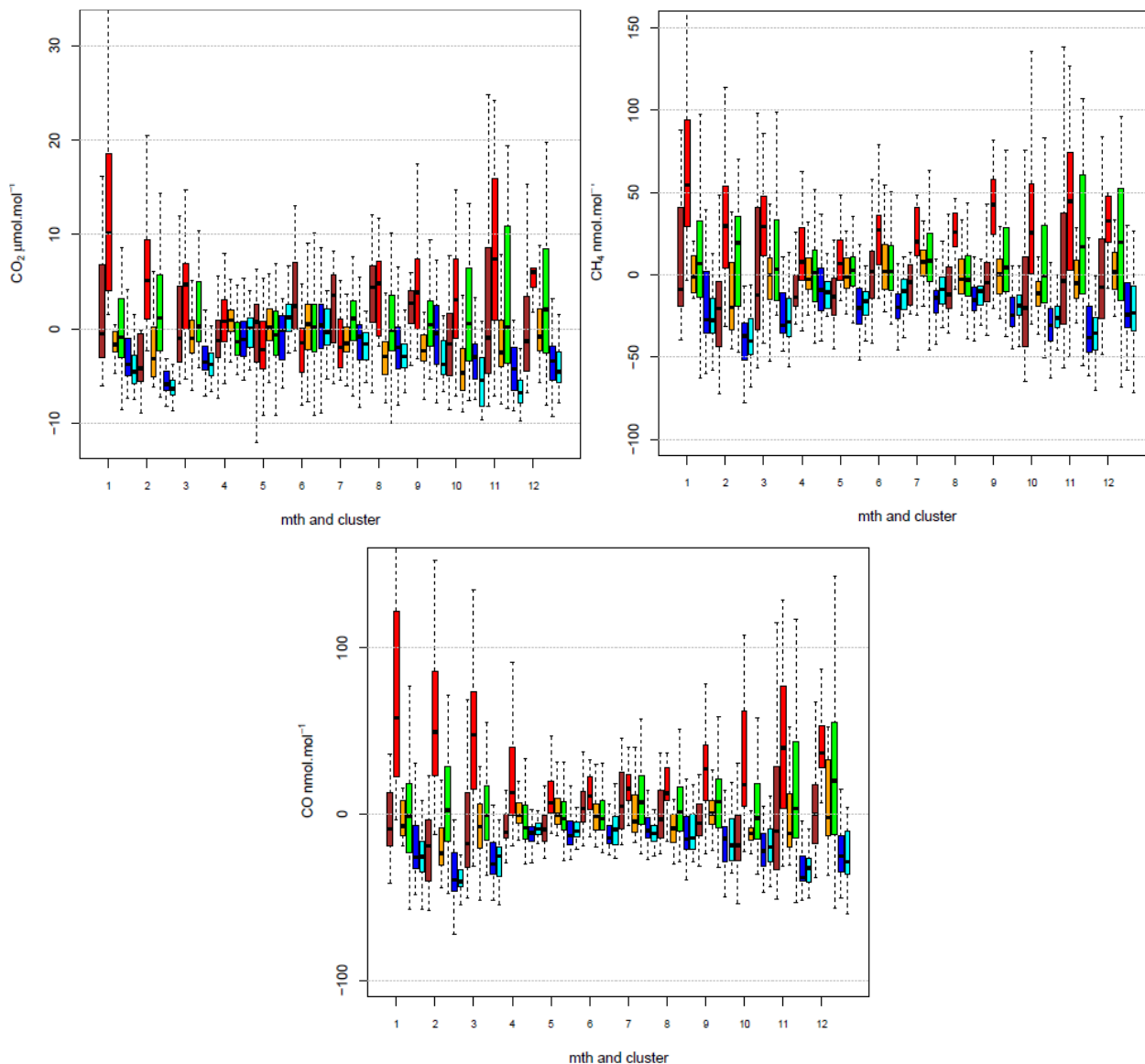
15 We analysed the 120m level residuals from the trend and seasonal cycle fitted curves with regard to air masses back-trajectories using the six clusters defined for the afternoon (see Figure 2). **Erreur ! Source du renvoi introuvable.** shows the boxplots of the residuals for each month and back-trajectories cluster. The boxplot displays the first and third quartile and the median of the residuals along with the overall data extension.

cluster	1		2		3		4		5		6	
	warm	cold	warm	cold	warm	cold	warm	cold	warm	cold	warm	cold
CO₂ / CH₄	0.21	0.92	0.33	0.89	0.01	0.84	0.47	0.86	0.18	0.8	0.24	0.87
CO₂ / CO	0.16	0.91	0.4	0.87	0.24	0.85	0.52	0.91	0.24	0.74	0.24	0.78
CH₄ / CO	0.74	0.93	0.87	0.84	0.71	0.87	0.76	0.92	0.75	0.85	0.78	0.88

20 **Table 8 Correlation coefficients between the compounds residuals for each cluster, split between a warm period from April to September and a cold period from October to March.**

The residuals of the three compounds are significantly stronger in the cold months than in the warm months. Clusters 5 (shown in blue) and 6 (in cyan) are associated with typical oceanic air masses with 96 hour back-trajectories reaching far over the Atlantic Ocean. These air masses are associated with the lowest variability of residuals (smallest boxplot extension). Negative

residuals are noticed year-round for CH₄ and CO and during the cold months for CO₂ (positive during warm months). Clusters 1 (brown) and 2 (red) are associated with southern and eastern trajectories. The associated residuals are much stronger and show large variabilities among the different synoptic situations with potential large deviations from the background.



5

Figure 12: Seasonal boxplot of the CO₂ (top left panel), CH₄ (top right panel) and CO residuals (bottom panel) at OPE 120m levels by cluster occurrence (cluster 1: brown, cluster 2 : red, cluster 3 : orange, cluster 4 : green, cluster 5 : blue, cluster 6 : cyan) for the period 2011-2018

10 Positive residuals are associated with Cluster 2 year-round for CH₄ and CO and during the cold months for CO₂. Cluster 3 (orange) is associated with either negative or positive residuals for the three compounds. Cluster 4 (green) is characterised by

relatively "stagnant " air masses with back-trajectories that do not extend far from the station in any particular directions. This type of air mass is associated with high residuals variability for the three compounds during the cold period. The residuals can be either positive or negative and show large spreads among the situations.

Erreur ! Source du renvoi introuvable. shows the correlation coefficients between the compounds residuals for each back-trajectory cluster, split between a warm period from April to September and a cold period from October to March. During the warm period, the correlation coefficients between CO₂ and either CH₄ or CO are low except for Cluster 4. However, the correlation coefficients between CH₄ and CO are around 0.75 for each cluster. During the cold period, the correlation coefficients between the different compounds are high and significant for every type of back-trajectory. Similar seasonal patterns for the CO₂/CO residuals and CO/CH₄ residuals were shown by Satar et al. (2016) in their two-year analysis of the Beromunster tower data in Switzerland.

Such patterns suggest that, during the cold months, the variations of three compounds are associated with the same anthropogenic processes convoluted through atmospheric dispersion. However, during the warm months, intraseasonal variations CO₂ residuals may have different drivers than CO or CH₄ residuals or their scale footprints are different. For example, natural biospheric contributions from different scales (local to continental) are larger for CO₂ during the warm months. Photochemical reactions are also much more activated during summertime. This result suggests that biospheric CO₂ fluxes may be the dominant driver of CO₂ intraseasonal variations during the warm period while anthropogenic emissions lead the intraseasonal variations of the three compounds during the cold period.

5. Conclusion

The OPE station is a new atmospheric station that was set up in 2011 as part of the ICOS Demo Experiment. It is a continental station sampling regionally representative air-masses. In addition to greenhouse gases and meteorological parameters mandatory for ICOS, the station measures aerosol properties and radioactivity and is part of the regional air quality network. The GHG measurements are performed in compliance with the ICOS atmospheric station specifications, and the station was labelled by ICOS in 2017. We have presented the GHG measurement system as well as the quality control performed. Next, analysis of the diurnal cycles, seasonal cycles and trends were given for the GHG data over the 2011-2018 period. Finally; we analysed the compounds residuals with regard to the air masse history.

The monthly mean field CMRs were estimated at between 0.01 and 0.04 ppm for CO₂, 0.14 and 0.5 ppb for CH₄ and 0.1 and 5.4 ppb for CO. The monthly mean field LTRs were estimated at between 0.003 and 0.013 ppm for CO₂, between 0.03 and 0.23 ppb for CH₄, and between 0.14 and 2.17ppb for CO. Biases estimated from the station working standards or by the "Cucumbers" intercomparison have been between ± 0.1 ppm for CO₂, ± 0.75 ppb for CH₄ and ± 5 ppb for CO since 2016.

The station was audited twice, just after its launch in 2011 and then in 2014. In 2011, the field audit revealed a median difference of 0.13 ppm for CO₂ and of 0.4 ppb for CH₄. During the 2014 audit, the mean biases were between 0.03 and 0.05

ppm for CO₂ and between 0.7 and 1.8 ppb for CH₄. The audits results along with the routine quality control metrics such as CMR, LTR and biases, and the “Cucumbers” intercomparisons showed that the OPE station met the compatibility goals defined by the WMO for CO₂, CH₄, and CO most of the time between 2011 and 2018 (WMO, 2018). The station set-up and its standard operating procedures are also fully compliant with the ICOS specifications (Laurent et al., 2017).

5 The diurnal cycles of the three compounds show amplification of the vertical gradient at night mainly caused by the night-time boundary layer stratification associated with ground cooling and radiative loss. Minimum values are reached during the afternoon when vertical mixing is more efficient. In addition to this main atmospheric dynamics influence, diurnal cycles of surface emissions and of photochemical processes also play some roles in the diurnal profiles of the three compounds. We focused on the afternoon data as we are interested in larger scale processes. We computed the mean seasonal cycles of CO₂,
10 CH₄ and CO. In addition relatively strong positive trends were observed for CO₂ and CH₄ with a mean annual growth rate of 2.4 ppm/year and 8.8 ppb/year respectively for the period 2011-2018. No significant trend was observed for CO. The residuals from the trends and seasonal cycles are much stronger during the cold period (October to March) than during the warm period (April to September). Our analysis of the residuals highlights the major influence of air masses on the atmospheric composition residuals. Air masses originating from the western quadrant with an Atlantic Ocean signature are
15 associated with the lowest residual variability. Eastern continental air masses or stagnant situations are associated with larger residuals and high variability. The correlations between the compounds residuals are also stronger during the cold period. Furthermore, there are no significant correlation between CO₂ and CO or CH₄ during the warm period.

Acknowledgements

20 The authors gratefully acknowledge the NOAA Air Resources Laboratory (ARL) for the provision of the HYSPLIT transport and dispersion model and READY website (<http://www.ready.noaa.gov>) used in this publication. S. Hammer from Heidelberg University and H. Aaltonen from FMI are thanked for their efforts during the OPE station audits. Staff from IRFU-CEA are acknowledged for their contribution to the station’s initial design and installation. We also thank staff from SNO-ICOS-France and from the ICOS Atmospheric Thematic Center for their technical support. The authors would like to thank the editor and
25 two anonymous referees who provided valuable suggestions and constructive comments to improve the manuscript.

Competing interests: The authors declare that they have no conflict of interest.

References

30 Bergamaschi, P., Karstens, U., Manning, A. J., Saunio, M., Tsuruta, A., Berchet, A., Vermeulen, A. T., Arnold, T., Janssens-Maenhout, G., Hammer, S., Levin, I., Schmidt, M., Ramonet, M., Lopez, M., Lavric, J., Aalto, T., Chen, H., Feist, D. G.,

- Gerbig, C., Haszpra, L., Hermansen, O., Manca, G., Moncrieff, J., Meinhardt, F., Necki, J., Galkowski, M., O'Doherty, S., Paramonova, N., Scheeren, H. A., Steinbacher, M., and Dlugokencky, E.: Inverse modelling of European CH₄ emissions during 2006–2012 using different inverse models and reassessed atmospheric observations, *Atmos. Chem. Phys.*, 18, 901–920, <https://doi.org/10.5194/acp-18-901-2018>, 2018
- 5
- Berhanu, T. A., Satar, E., Schanda, R., Nyfeler, P., Moret, H., Brunner, D., Oney, B., and Leuenberger, M.: Measurements of greenhouse gases at Beromünster tall-tower station in Switzerland, *Atmos. Meas. Tech.*, 9, 2603–2614, <https://doi.org/10.5194/amt-9-2603-2016>, 2016
- 10
- Broquet, G., Chevallier, F., Bréon, F.-M., Kadyrov, N., Alemanno, M., Apadula, F., Hammer, S., Haszpra, L., Meinhardt, F., Morguí, J. A., Necki, J., Piacentino, S., Ramonet, M., Schmidt, M., Thompson, R. L., Vermeulen, A. T., Yver, C., and Ciais, P.: Regional inversion of CO₂ ecosystem fluxes from atmospheric measurements: reliability of the uncertainty estimates, *Atmos. Chem. Phys.*, 13, 9039–9056, <https://doi.org/10.5194/acp-13-9039-2013>, 2013.
- 15
- Carslaw DC, Ropkins K : openair — An R package for air quality data analysis. *Environmental Modelling & Software*, 27–28(0), 52–61, 2012
- El Yazidi, A., Ramonet, M., Ciais, P., Broquet, G., Pison, I., Abbaris, A., Brunner, D., Conil, S., Delmotte, M., Gheusi, F., Guerin, F., Hazan, L., Kachroudi, N., Kouvarakis, G., Mihalopoulos, N., Rivier, L., and Serça, D.: Identification of spikes associated with local sources in continuous time series of atmospheric CO, CO₂ and CH₄, *Atmos. Meas. Tech.*, 11, 1599–1614, <https://doi.org/10.5194/amt-11-1599-2018>, 2018.
- Hammer, S., Konrad, G., Vermeulen, A. T., Laurent, O., Delmotte, M., Jordan, A., Hazan, L., Conil, S., and Levin, I.: Feasibility study of using a "travelling" CO₂ and CH₄ instrument to validate continuous in situ measurement stations, *Atmos. Meas. Tech.*, 6, 1201–1216, <https://doi.org/10.5194/amt-6-1201-2013>, 2013
- 25
- Hazan, L., Tarniewicz, J., Ramonet, M., Laurent, O., and Abbaris, A.: Automatic processing of atmospheric CO₂ and CH₄ mole fractions at the ICOS Atmosphere Thematic Centre, *Atmos. Meas. Tech.*, 9, 4719–4736, <https://doi.org/10.5194/amt-9-4719-2016>, 2016
- 30
- Heid, L., Calvaruso, C., Andrianantenaina, A. Granier A., Conil S., Rathberger C., Turopault M.P., Longdoz B. : Seasonal time-course of the above ground biomass production efficiency in beech trees (*Fagus sylvatica* L.). *Annals of Forest Science* 75: 31. <https://doi.org/10.1007/s13595-018-0707-9>, 2018

- Kadyrov, N., Broquet, G., Chevallier, F., Rivier, L., Gerbig, C., and Ciais, P.: On the potential of the ICOS atmospheric CO₂ measurement network for estimating the biogenic CO₂ budget of Europe, *Atmos. Chem. Phys.*, 15, 12765-12787, <https://doi.org/10.5194/acp-15-12765-2015>,
- 5 Kountouris, P., Gerbig, C., Rödenbeck, C., Karstens, U., Koch, T. F., and Heimann, M.: Atmospheric CO₂ inversions on the mesoscale using data-driven prior uncertainties: quantification of the European terrestrial CO₂ fluxes, *Atmos. Chem. Phys.*, 18, 3047-3064, <https://doi.org/10.5194/acp-18-3047-2018>, 2018
- Kromer B., Münnich K.O.: CO₂ Gas Proportional Counting in Radiocarbon Dating — Review and Perspective. In: Taylor
10 R.E., Long A., Kra R.S. (eds) *Radiocarbon After Four Decades*. Springer, New York, NY, 1992
- Laurent, O.: ICOS Atmospheric Station Specifications, ICOS technical report (publicly available on https://icos-atc.lscce.ipsl.fr/doc_public), 2017
- 15 Le Quéré, C. and coauthors: Global Carbon Budget 2018, *Earth System Science Data*, 10, 1-54, 2018, DOI: 10.5194/essd-10-2141-2018
- Lebegue, B., Schmidt, M., Ramonet, M., Wastine, B., Yver Kwok, C., Laurent, O., Belviso, S., Guemri, A., Philippon, C., Smith, J., and Conil, S.: Comparison of nitrous oxide (N₂O) analyzers for high-precision measurements of atmospheric mole
20 fractions, *Atmos. Meas. Tech.*, 9, 1221-1238, <https://doi.org/10.5194/amt-9-1221-2016>, 2016
- Leip A, Skiba U, Vermeulen A, Thompson RL.: A complete rethink is needed on how greenhouse gas emissions are quantified for national reporting. *Atmospheric Environment*. 174:237-240. <https://doi.org/10.1016/j.atmosenv.2017.12.006>; 2018
- 25 Levin, I., Münnich, K., Weiss, W.: The Effect of Anthropogenic CO₂ and 14C Sources on the Distribution of 14C in the Atmosphere. *Radiocarbon*, 22(2), 379-391. doi:10.1017/S003382220000967X,1980
- Lopez, M., Schmidt, M., Ramonet, M., Bonne, J.-L., Colomb, A., Kazan, V., Laj, P., and Pichon, J.-M.: Three years of semicontinuous greenhouse gas measurements at the Puy de Dôme station (central France), *Atmos. Meas. Tech.*, 8, 3941-
30 3958, <https://doi.org/10.5194/amt-8-3941-2015>, 2015
- Lowry D., Lanoisellé M.E., Fisher R. E., Martin M., Fowler C. M. R., France J. L., Hernández-Paniagua I. Y., Novelli P.C., Sriskantharajah S., O'Brien P., Rata N.D., Holmes C.W., Fleming Z. L., Clemitshaw K. C., Zazzeri G., Pommier M., McLinden

- C. A. and Nisbet E.G.: Marked long-term decline in ambient CO mixing ratio in SE England, 1997–2014: evidence of policy success in improving air quality. *Sci. Rep.* 6, 25661; doi: 10.1038/srep25661, 2016
- Nisbet, E. G., Manning, M. R., Dlugokencky, E. J., Fisher, R. E., Lowry, D., Michel, S. E., et al: Very strong atmospheric methane growth in the 4 years 2014–2017: Implications for the Paris Agreement. *Global Biogeochemical Cycles*, 33. <https://doi.org/10.1029/2018GB006009>, 2019
- Novelli, P. C., Masarie, K. A., Lang, P. M., Hall, B. D., Myers, R. C., and Elkins, J. W. (2003), Reanalysis of tropospheric CO trends: Effects of the 1997–1998 wildfires, *J. Geophys. Res.*, 108, 4464, doi:10.1029/2002JD003031, D15
- 10 Peters, G. P., Le Quééré, C., Andrew, R. M., Canadell, J. G., Friedlingstein, P., Ilyina, T., Jackson, R. B., Joos, F., Korsbakken, J. I., McKinley, G. A., Sitch, S., and Tans, P.: Towards real-time verification of CO₂ emissions, *Nat. Clim. Change*, 7, 848–850, <https://doi.org/10.1038/s41558-017-0013-9>, 2017
- 15 Pison, I., Berchet, A., Saunio, M., Bousquet, P., Broquet, G., Conil, S., Delmotte, M., Ganesan, A., Laurent, O., Martin, D., O'Doherty, S., Ramonet, M., Spain, T. G., Vermeulen, A., and Yver Kwok, C.: How a European network may help with estimating methane emissions on the French national scale, *Atmos. Chem. Phys.*, 18, 3779–3798, <https://doi.org/10.5194/acp-18-3779-2018>, 2018
- 20 Rella, C. W., Chen, H., Andrews, A. E., Filges, A., Gerbig, C., Hatakka, J., Karion, A., Miles, N. L., Richardson, S. J., Steinbacher, M., Sweeney, C., Wastine, B., and Zellweger, C.: High accuracy measurements of dry mole fractions of carbon dioxide and methane in humid air, *Atmos. Meas. Tech.*, 6, 837–860, <https://doi.org/10.5194/amt-6-837-2013>, 2013
- Satar, E., Berhanu, T. A., Brunner, D., Henne, S., and Leuenberger, M.: Continuous CO₂/CH₄/CO measurements (2012–2014) at Beromünster tall tower station in Switzerland, *Biogeosciences*, 13, 2623–2635, <https://doi.org/10.5194/bg-13-2623-2016>, 2016
- 25 Schibig, M. F., Steinbacher, M., Buchmann, B., van der Laan-Luijkx, I. T., van der Laan, S., Ranjan, S., and Leuenberger, M. C.: Comparison of continuous in situ CO₂ observations at Jungfraujoch using two different measurement techniques, *Atmos. Meas. Tech.*, 8, 57–68, <https://doi.org/10.5194/amt-8-57-2015>, 2015
- 30

- Schmidt, M., Lopez, M., Yver Kwok, C., Messenger, C., Ramonet, M., Wastine, B., Vuillemin, C., Truong, F., Gal, B., Parmentier, E., Cloué, O., and Ciais, P.: High-precision quasi-continuous atmospheric greenhouse gas measurements at Trainou tower (Orléans forest, France), *Atmos. Meas. Tech.*, 7, 2283-2296, <https://doi.org/10.5194/amt-7-2283-2014>, 2014
- 5 Sen, P.K.: Estimates of the regression coefficient based on Kendall's tau, *Journal of the American Statistical Association*, 63 (324): 1379–1389, doi:10.2307/2285891, 1968.
- Thoning, K.W., P.P. Tans, and W.D. Komhyr, Atmospheric carbon dioxide at Mauna Loa Observatory, 2. Analysis of the NOAA/GMCC data, 1974 1985., *J. Geophys. Res.*, 94, 8549 8565, 1989
- 10 Vardag, S. N., Hammer, S., O'Doherty, S., Spain, T. G., Wastine, B., Jordan, A., and Levin, I.: Comparisons of continuous atmospheric CH₄, CO₂ and N₂O measurements – results from a travelling instrument campaign at Mace Head, *Atmos. Chem. Phys.*, 14, 8403-8418, <https://doi.org/10.5194/acp-14-8403-2014>, 2014
- 15 Turner, A.J., Frankenberg, C., Kort, E.A.: Interpreting contemporary trends in atmospheric methane, *Proc. Natl. Acad. Sci.*, 116 (8) 2805-2813; DOI: 10.1073/pnas.1814297116, 2019
- Vermeulen, A. T., Hensen, A., Popa, M. E., van den Bulk, W. C. M., and Jongejan, P. A. C.: Greenhouse gas observations from Cabauw Tall Tower (1992–2010), *Atmos. Meas. Tech.*, 4, 617-644, <https://doi.org/10.5194/amt-4-617-2011>, 2011
- 20 WMO: 19th WMO/IAEA Meeting on Carbon Dioxide, Other Greenhouse Gases and Related Tracers Measurement Techniques (GGMT-2017), Dübendorf, Switzerland, 27-31 August 2017, GAW Report No.242, World Meteorological Organization, Geneva, Switzerland, 2018
- Yuan, Y., Ries, L., Petermeier, H., Trickl, T., Leuchner, M., Couret, C., Sohmer, R., Meinhardt, F., and Menzel, A.: On the diurnal, weekly, and seasonal cycles and annual trends in atmospheric CO₂ at Mount Zugspitze, Germany, during 1981–2016, *Atmos. Chem. Phys.*, 19, 999-1012, <https://doi.org/10.5194/acp-19-999-2019>, 2019
- Yver Kwok, C., Laurent, O., Guemri, A., Philippon, C., Wastine, B., Rella, C. W., Vuillemin, C., Truong, F., Delmotte, M., Kazan, V., Darding, M., Lebègue, B., Kaiser, C., Xueref-Rémy, I., and Ramonet, M.: Comprehensive laboratory and field testing of cavity ring-down spectroscopy analyzers measuring H₂O, CO₂, CH₄ and CO, *Atmos. Meas. Tech.*, 8, 3867-3892, <https://doi.org/10.5194/amt-8-3867-2015>, 2015.
- 30

Zellweger, C., Hüglin, C., Klausen, J., Steinbacher, M., Vollmer, M., and Buchmann, B.: Inter-comparison of four different carbon monoxide measurement techniques and evaluation of the long-term carbon monoxide time series of Jungfraujoch, *Atmos. Chem. Phys.*, 9, 3491-3503, 2009.

- 5 Zellweger, C., Emmenegger, L., Firdaus, M., Hatakka, J., Heimann, M., Kozlova, E., Spain, T. G., Steinbacher, M., van der Schoot, M. V., and Buchmann, B.: Assessment of recent advances in measurement techniques for atmospheric carbon dioxide and methane observations, *Atmos. Meas. Tech.*, 9, 4737-4757, <https://doi.org/10.5194/amt-9-4737-2016>, 2016